

ANALYSIS OF THE FEASIBILITY OF BATTERY ENERGY STORAGE AS THE SOLUTION FOR ELECTRICITY GRID CONGESTION

A thesis submitted to the Delft University of Technology in partial fulfillment
of the requirements for the degree of

Master of Science in Sustainable Energy Technologies

by

Stijn Hartman

November 15, 2022

Stijn Hartman: *Analysis of the feasibility of battery energy storage as the solution for electricity grid congestion* (2022)

The work in this thesis was made in the:

DC systems, Energy conversion and Storage
Sustainable Energy Technologies
Electrical Engineering, Mathematics and Computer Science
Delft University of Technology

Thesis Committee: Prof. dr. ir. Pavol Bauer
Dr. ir. Laura Ramirez Elizondo
Dr. ir. Pedro Vergaro Barrios

ABSTRACT

The increasing share of intermittent renewable energy sources and the electrification of the energy system are causing challenges for the electricity grid. These developments lead to a less controllable and more decentralized energy generation portfolio, which require far-reaching adaptations of the electricity grid. Although adaptations are realized, the pace is too slow, which results in temporary shortages of capacity of the grid, called congestion. Thus, other solutions to increase the flexibility of the grid are required.

Battery energy storage systems (BESSs) are currently seen as a promising solution to increase the flexibility of the grid and to relieve congestion. Nevertheless, solely using a BESS to relieve congestion is not an economic feasible solution. There are multiple applications for BESSs in the electricity grid. To make the business cases financially viable, several applications have to be combined. Therefore, this research aims to evaluate the possibility of developing a financially viable business case for a BESS that effectively relieves congestion, while generating profit on Dutch electricity markets. The markets that are investigated are the Frequency Curtailment Reserve market and the imbalance market. Since these markets are considered as most promising for the application of BESSs.

To investigate the feasibility four mathematical optimization problems are formulated, applying (Mixed Integer) Linear Programming. These models assess the sizing and profit generating properties of a congestion relieving BESS, while pursuing different objectives. The first two models determine the optimal size and market participation, considering perfect foresight of the market prices and load profile. Where the first of these two models pursues minimal investment costs for the BESS, the second model pursues maximal total profit. The other two models consider uncertainty in price and load forecasts. The other two models consider uncertainty in price and load forecasts. The first of these two models optimizes the BESS for minimal investment, considering uncertainties. The second model optimizes for maximum profit. Furthermore, the second model introduces a risk factor, which is investigated through the Conditional Value at Risk (CVaR).

Thereafter, the feasibility of the solution is investigated through three case studies. The case studies are based on three nodes of the distribution grid for which the Dutch Distribution System Operator Liander forecasts structural congestion in the future.

The study shows that for two of the three case studies a profitable business case can be theoretically accomplished. The congestion in the third case study is too severe to generate a profitable business case without monetary compensation for the relieving of congestion. Furthermore, the results show that a shorter payback time of the investment does not always mean a more profitable business case, as battery degradation plays an important role. The two models that incorporate uncertainty of the forecasts show that a relatively higher uncertainty has relatively higher negative effects on the profitability of the BESS. The results of the model, that introduces the CVaR, provide an insight on the effect of monetary risk on the profitability of the BESS. The results show an increasing tendency of the profitability as risk is permitted. However, the largest increase in profitability is realized by allowing only a small risk factor. This increasing tendency continues at a lower rate as more risk is allowed. Additionally, it should be considered that the profitability in all cases is heavily dependent on the quality of the trading strategy and the accuracy of the forecasts.

ACKNOWLEDGEMENTS

This thesis was written in partial fulfillment of the requirements for the degree of Master of Science in Sustainable Energy Technologies at the Delft University of Technologies. This thesis is the final stage in the completion of my degree and therefore marks the end of my academic career.

I would like to express my gratitude towards a number of people who have contributed to this project. First of all, I would like to thank my thesis supervisor Dr. ir. Laura Ramirez Elizondo for guiding me during this project and letting me conduct research into this interesting topic. I would also like to express my gratitude towards Prof. Dr. ir. Pavol Bauer and Dr. ir. Pedro Vergaro Barrios for sparing the time to evaluate my work as thesis committee members.

Furthermore, I would like to thank Lars Rupert and Ruud Nijs as they gave me the opportunity to research this topic at their company Giga Storage. Besides them I would like to thank the entire Giga Storage team for welcoming me and supporting me during this project. I have truly enjoyed my time as a thesis intern at Giga Storage and learned a lot from all the inspiring colleagues.

In conclusion, I would like to express my gratitude towards my parents, my family, and my friends as they always provided me with immense support and helped me enjoy my time at the TU Delft to the fullest.

Stijn Hartman
November 15, 2022
Delft

TABLE OF CONTENTS

List of Figures	vi
List of Tables	viii
Nomenclature	ix
1 INTRODUCTION	1
2 THEORETICAL BACKGROUND	4
2.1 Congestion on the Electricity Grid	4
2.2 Energy Storage Technology	5
2.2.1 Battery Energy Storage Systems	6
2.2.2 Battery Energy Storage System Setup	8
2.2.3 Battery Energy Storage System Lifetime Evaluation	9
2.3 Electricity Grid	10
2.3.1 Electricity Cables	11
2.3.2 Electricity Substations	11
2.4 Electricity Markets	12
2.4.1 Market Outline	12
2.4.2 Day-Ahead Market	13
2.4.3 Intraday Market	13
2.4.4 Frequency Containment Reserve	14
2.4.5 Frequency Restoration Reserve	14
2.4.6 Passive or Voluntary Balancing Market	15
2.4.7 Potential of BESS on the Electricity Markets	15
2.5 Optimization Programming	16
3 LITERATURE REVIEW	17
4 MODEL FORMULATION	19
4.1 Methodology	19
4.2 Perfect Foresight Model Formulations	19
4.2.1 Minimum Investment Model	19
4.2.2 Maximum Profit Model	23
4.3 Uncertainty Based Optimisation Models	23
4.3.1 Uncertainty Based Programming Methodology	23
4.3.2 Uncertainty Minimum Investment Model	24
4.3.3 Risk-Based Maximum Profit Model	26
4.3.4 Lifetime Evaluation	28
5 CASE STUDIES AND DATA ANALYSIS	30
5.0.1 Overview of the Case Studies	30
5.0.2 Uncertain Load Data	34
5.0.3 Electricity Price Data	35
6 RESULTS	36
6.1 Minimum Investment Model	36
6.2 Maximum Profit Model	39
6.3 Model Comparison	41
6.4 Uncertainty Minimum Investment Model	42
6.5 Risk-Based Maximum Profit Model	43
7 DISCUSSION	46
7.1 Minimum Investment Model Analysis	46
7.2 Maximum Profit Model Analysis	47
7.3 Uncertainty minimum investment Model Analysis	48
7.4 Risk-Based Maximum Profit Analysis Model	48
8 CONCLUSION	50
9 RECOMMENDATIONS	52
Bibliography	54

LIST OF FIGURES

Figure 2.1	Transport capacity charts for the Dutch electricity grid on 09-06-2022[1].	5
Figure 2.2	Comparison of power density, energy density, efficiency, costs and lifetime for the most popular Li-ion battery storage technologies for Grid applications: (a) Lithium Iron Phosphate, (b) Lithium Nickel Manganese Cobalt Oxide, (c) Lithium Nickel Cobalt Aluminum Oxide - author's elaboration from [2], [3] and [4]	7
Figure 2.3	Battery Energy Storage System schematics and setup of the main components [2].	8
Figure 2.4	Electricity grids in the Netherlands.	10
Figure 2.5	Layout of the electricity grid [5].	11
Figure 2.6	Layout of the electricity markets.	13
Figure 2.7	Overview of the balancing process [6].	14
Figure 4.1	Normal Distribution [7].	24
Figure 4.2	Conversion of probability density function to discrete levels [8].	25
Figure 4.3	Example of the rainflow counting algorithm.	28
Figure 5.1	Overview of the IJpolder congestion area [9].	31
Figure 5.2	Load and capacity on IJpolder transmission station.	31
Figure 5.3	Overview of the Terschelling congestion area [10].	32
Figure 5.4	Load and capacity on Terschelling transmission station.	32
Figure 5.5	Overview of the Westhaven congestion area [11].	33
Figure 5.6	Load and capacity on Westhaven transmission station.	33
Figure 5.7	Average market prices for the high, medium and low scenarios in 2026.	35
Figure 5.8	Average market prices for the high, medium and low scenarios in 2030.	35
Figure 6.1	BESS output for the first month of the IJpolder case study with the minimum investment model.	37
Figure 6.2	BESS output for the first month of the Terschelling case study with the minimum investment model.	37
Figure 6.3	BESS output for the first month of the Westhaven case study with the minimum investment model.	38
Figure 6.4	Capacity fading of the BESS for the IJpolder case study with the minimum investment model.	38
Figure 6.5	Capacity fading of the BESS for the Terschelling case study with the minimum investment model.	38
Figure 6.6	Capacity fading of the BESS for the Westhaven case study with the minimum investment model.	39
Figure 6.7	BESS output for the first month of the IJpolder case study with the maximum profit model.	40
Figure 6.8	BESS output for the first month of the Terschelling case study with the maximum profit model.	40
Figure 6.9	BESS output for the first month of the Westhaven case study with the maximum profit model.	40
Figure 6.10	Capacity fading of the BESS for the IJpolder case study with the maximum profit model.	41
Figure 6.11	Capacity fading of the BESS for the Terschelling case study with the maximum profit model.	41
Figure 6.12	Capacity fading of the BESS for the Westhaven case study with the maximum profit model.	41
Figure 6.13	Results of the risk-based maximum profit model for the first month of the IJpolder scenario.	44

Figure 6.14	Results of the risk-based maximum profit model for the first month of the Terschelling scenario.	44
Figure 6.15	Results of the risk-based maximum profit model for the first half year of the Westhaven scenario.	44
Figure 6.16	Change in values for different risk levels for the first half year of the Westhaven case study.	45

LIST OF TABLES

Table 2.1	Comparison of different battery technologies.	7
Table 2.2	Overview of different electricity cables [5]	11
Table 2.3	Overview of the different substations[5]	12
Table 5.1	Important numbers at station IJpolder in 2026.	31
Table 5.2	Important numbers at station Terschelling in 2030.	33
Table 5.3	Important numbers at station Westhaven in 2026.	34
Table 5.4	Probability of the different load scenarios	34
Table 6.1	Parameters used in the different models.	36
Table 6.2	The results from the minimum investment model	37
Table 6.3	The results from the maximum profit model.	39
Table 6.4	Comparison of the minimum investment model and the maximum profit model.	42
Table 6.5	The results from the minimum investment model while considering uncertainty.	42
Table 6.6	The results from the maximum profit model without considering uncertainty.	43
Table 7.1	Summary of important number for the minimum investment model	47
Table 7.2	Summary of the financial results of the maximum investment model.	48

NOMENCLATURE

List of Abbreviations

<i>BESS</i>	Battery Energy Storage System
<i>BMS</i>	Battery Management System
<i>BRP</i>	Balance Responsible Party
C_{cal}	Calendar Capacity Fading
C_{cyc}	Cycling Capacity Fading
$C_{rampFCR}$	Ramp Cost FCR Market
C_{ramp}	Ramp Cost Imbalance Market
$Capex^E$	Capital Expenditure for Energy Capacity
$Capex^P$	Capital Expenditure for Power Capacity
<i>cd</i>	Cycle Depth
<i>CVaR</i>	Conditional Value at Risk
<i>d</i>	Binary Dummy Variable
<i>DSO</i>	Distribution System Operator
E^{BESS}	Nameplate Energy Capacity Battery
<i>EMS</i>	Energy Management System
<i>f</i>	Index for FCR Price Scenario
<i>FCR</i>	Frequency Containment Reserves
<i>FRR</i>	Frequency Restoration Reserves
<i>GHG</i>	Green House Gas
<i>i</i>	Index for Imbalance Price Scenario
<i>IGBT</i>	Insulated-Gate Bipolar Transistor
<i>IGCC</i>	International Grid Control Cooperation
<i>ISP</i>	Imbalance Settlement Period
<i>l</i>	Index for Load Scenario
<i>LFP</i>	Lithium Iron Phosphate-based
<i>Li – ion</i>	Lithium-ion
<i>LP</i>	Linear Programming
<i>MILP</i>	Mixed Integer Linear Programming
<i>NaNiCl2</i>	Sodium-Nickel-Chloride
<i>NaS</i>	Sodium-sulfur

nc	Number of Cycles
NCA	Nickel Cobalt Aluminum Oxide-based
NMC	Nickel Manganese Cobalt Oxide- based
p^{BESS}	Nameplate Power Capacity Battery
$p^{Capacity}$	Power Capacity of Grid Node
p^{Chr}	Battery Power Charging
p^{Dis}	Battery Power Discharging
p^{FCR}	Power Capacity offered on FCR market
p^{load}	Load on Grid Node
$PB - Acid$	Lead-acid
RES	Renewable Energy Sources
SoC	State of Charge
T	Temperature
t	Time
TSO	Transmission System Operator
VaR	Value at Risk
$VRFB$	Vanadium redox flow battery
z	Frequency Containment Reserves timestep
$z_{f,i,l}$	Auxiliary Variable for CVaR Linearisation

List of Greek Symbols

β	Confidence Interval
ϵ	Value at Risk Threshold
η	Efficiency Battery Energy Storage System
λ^{FCR}	Electricity Price FCR market
λ^{Imb}	Electricity Price Imbalance market
ω	Risk Factor
π	Loss for BESS owner
σ	Standard Deviation
θ	Investment cost of storage
ζ	Profit from Market Operations
ζ	Probability of Occurance of a Scenario

In 2019, the Dutch government along many organisations and companies signed the Climate Act, this sets legally binding targets to reduce greenhouse gas (GHG) emissions by 49% by 2030 and by 95% by 2050 (compared to 1990 levels) and for 100% of electricity to come from Renewable Energy Sources (RES) by 2050. The Dutch government has already taken action in the regard; the transition has been initiated in many industries and will pick up pace considerably over the coming years. This is demonstrated by the fact that in 2020, 11.1% of the total Dutch energy consumption came from renewable resources, while this share was only 8.8% in 2019.

In addition to the increasing share of renewable energy, another effect of the energy transition is the electrification of the entire energy system. Due to beneficial policies the amount of electric cars is increasing and the electrification of industry processes is seen as one of the most promising transition pathways. The Dutch government is making great efforts to work towards a more sustainable energy system, and a transition of this scale and complexity is inevitably coupled with difficulties along the way. For example, the Dutch grid is facing major capacity problem during the energy transition. Daan Schut, chief transition officer at network operator Alliander, has said: 'In recent years we have looked too much at sustainable energy and too little at the infrastructure [12].'

The increasing adaptation of renewable energy in the electricity sector leads to an more and more decentralized generation portfolio, requiring far-reaching adaptations to the transmission and distribution grids. However, the grid does not expand as fast as the renewable distributed generation capacity, resulting in a shortage of capacity of the electricity grid, known as congestion. Furthermore, conventional power plants used to be located near major demand sites, while a great share of renewable energy capacity is located far from areas of high demand. In countries, with high adoption of renewable energy this causes an increasing amount of grid congestion both in the transmission and distribution grid. The grid congestion results in curtailment of renewable energy sources and an increasing problem to admit new companies to the electricity grid. This leads to both environmental and economic consequences, as an increasing amount of potentially generated electricity from renewable energy sources, a clean resource and basically free of marginal costs remains unused[13].

This problem also occurs in the Dutch electricity grid and this demands more and more flexibility of the electricity grid. Studies have shown that the power grid can absorb variation and uncertainty from direct integration of renewable energy generation up to 10% of the system installed capacity without major technical problems or substantial additional costs [14]. However, large-scale renewable energy integration can cause heavier and more frequent mismatches between supply and demand.

There are many different possibilities to increase the flexibility of the grid, one being energy storage. Energy storage is promising because it enables the decoupling of supply and demand by time-shifting the delivery of power, thus allowing temporary mismatches between supply and demand. Furthermore, the peak-shaving abilities are necessary to ensure the stability of the future grid. In this thesis energy storage is investigated as a possible solution to relieve congestion.

Among all different energy storage technologies, this thesis focuses on Battery Energy Storage Systems (BESSs). BESSs are well suited to relieve congestion, as they have high efficiency and fast response time. BESS technology is progressively adopted across the European energy market. There

are many different use cases for BESSs and due to increasing opportunities in various markets and the decreasing capital costs of batteries, these use cases are explored intensively. These cases include, for example, grid services, power quality control, energy arbitrage and congestion relief. To create a profitable business case for the owner of a BESS, it is imperative to stack multiple business cases [15]. Therefore, the stacking of different use cases is researched extensively [16].

From the literature it becomes clear that solutions for congestion are a necessity and that BESSs are a feasible solution. Nevertheless, the stacking of different use cases is required to obtain a profitable business case. Therefore, the objective of this thesis is to investigate the possibility of creating a profitable business case for a BESS that relieves local congestion while generating profit on Dutch electricity markets. The markets that are investigated are the Frequency Containment Reserve (FCR) market and the imbalance market, as these are seen as promising opportunities for BESSs [17].

In support of the objective of this thesis, a research question is formulated. This is the starting point and guideline of this thesis. The research question is formulated as follows:

- Is it possible to create a profitable business case for a grid connected BESS that relieves local congestion on the Dutch electricity grid, while generating profit through market operations?

Answering this question is the main goal of this thesis. Nevertheless, in order to do so sub-questions have to be formulated and answered. The following sub-questions are formulated to support answering the main research question:

- Is it possible to develop a model that optimises the size of a BESS to relieve congestion, while generating revenue on the electricity market?
- What is the influence of the severity of the congestion on the profitability of a congestion relieving BESS?
- What is the influence of uncertainty in market and load forecasts on the sizing and revenue of a BESS?
- What is the influence of monetary risks taken by the BESS owner on the sizing and revenue of a BESS?

To answer the questions this thesis is structured in the following way. In chapter 2, theoretical background is provided on the different aspects of the problem, such as congestion, the electricity grid, battery energy storage system and the electricity market. The goal of this chapter is to gain a deeper understanding of the different aspects of this problem.

Thereafter, chapter 3 provides a literature review on the subject of this thesis. This chapter gives an overview of the existing literature and formulates the knowledge gap.

Chapter 4 provides the description of four different linear programming optimisation models to assess the sizing and profit generating properties of a congestion relieving BESS, while pursuing different objectives. The first two models are based on perfect forecasting and the second two factor in uncertainties in the forecasting of the load and the market prices.

Furthermore, in chapter 5 the different case studies are presented. The cases are described and the data is visualized. The chapter also describes the way the uncertainty of the load forecasting is modeled.

In chapter 6 the results of the different models and the different case studies are presented. The results of the different models are compared.

Chapter 7, provides an analysis of the results. Each model is discussed and an interpretation of the finding is given.

A conclusion of the thesis is presented in chapter 8. The answers to the different research question is presented.

Chapter 9, is the final chapter of this thesis. In this chapter recommendations on further research on this subject is presented. The recommendations are based on the knowledge and experience gained through this thesis.

2

THEORETICAL BACKGROUND

This chapter presents the theoretical background that is required to understand this thesis. The chapter aims to broaden the general understanding of the reader on this complex subject. Section 2.1 discusses the effects of congestion and the reasons for congestion. In section 2.2 theoretical background is provided on battery energy storage systems. Section 2.3 provides an overview of the Dutch electricity grid and its most important parts. Furthermore, section 2.4 describes the European energy market and the different market mechanisms existing. Lastly, section 2.5 discusses and explains optimisation programming.

2.1 CONGESTION ON THE ELECTRICITY GRID

This sections aims to provide a detailed description of congestion and why this topic is becoming more and more relevant. Furthermore, this section describes the problems that occur as a result of congestion.

The increasing adoption of intermittent RES and the decentralisation of the generation portfolio results in capacity problems of the grid. As the grid does not expand as fast as the renewable distributed generation capacity. In countries, with high adoption of renewable energy, an increasing amount of grid congestion, both in the transmission and distribution grid, occurs. The grid congestion results in curtailment of renewable energy sources and an increasing problem to admit new users to the electricity grid. This problem has both environmental and economic consequences, as an increasing amount of potentially generated electricity from renewable energy sources, a clean resource and basically free of marginal costs, remains unused [13].

This thesis focuses on the Dutch electricity grid. Congestion forms a big problem for the Dutch Transmission System Operator (TSO) and for the Distribution System Operators (DSOs). Figure 2.1 shows two charts of the transport capacity of the Dutch electricity grid. Figure 2.1a shows the capacity for feeding in energy and figure 2.1b shows the capacity for taking off energy. The parts covered in red indicate regions where structural congestion occurs. In this regions new requests for transport capacity will be denied. In the orange regions structural congestion is being announced at the Authority for Consumers and Markets. Furthermore, in the yellow regions transport capacity scarcity threatens and an altered quotation regime is in place. In the rest of the map no capacity scarcity exists yet. It is clear from the figures that congestion forms a problem in the Netherlands. The absence of sufficient transport capacity prevents the implementation of more renewable energy sources, which are required to reach the goals stated in the Paris Agreement.

Additionally, the Dutch TSO TenneT deals with high costs as a result of congestion. In case of congestion the transportation of renewable energy to region with high demand is limited. Therefore, TenneT has to offer power plants, near the energy demand, a monetary compensation to meet the demand in this area. This energy is more expensive than the cheap energy from RES, which in this case has to be curtailed. In the past, congestion lasted a view hours in the worst case, nowadays this periods can be as long as 14 hours a day. In 2021, the costs for TeneT as a result of congestion were 340 million euros, while in 2020 this costs were merely 78 million euros. These costs are paid by the consumer, thus the increase of amount of congestion results in higher electricity bills for the end-users [18].

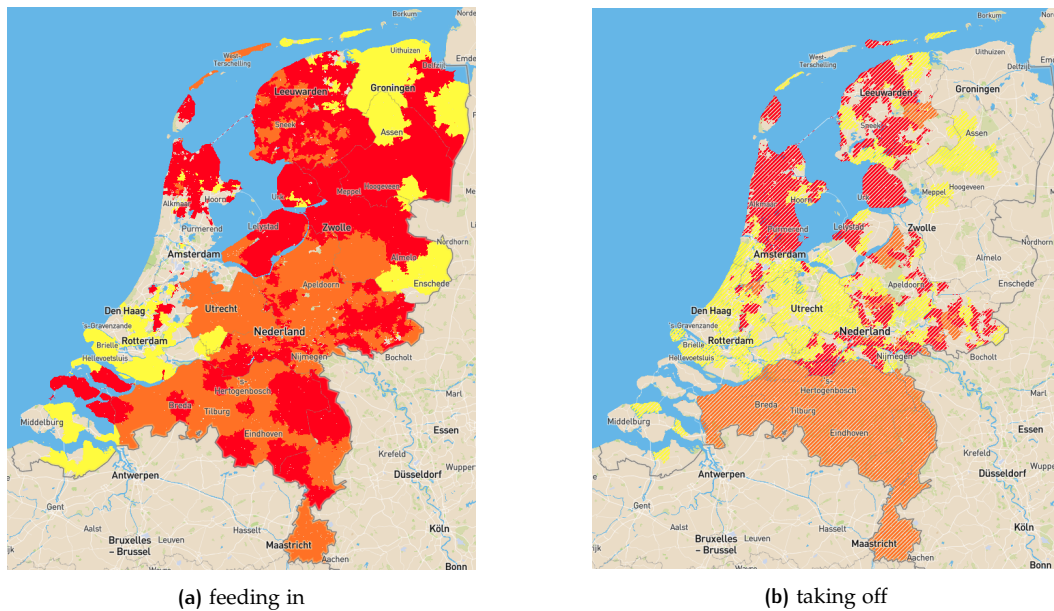


Figure 2.1: Transport capacity charts for the Dutch electricity grid on 09-06-2022[1].

In the literature different solutions for congestion are discussed. Firstly, congestion management is commonly proposed, as by Blijswijk and de Vries [19]. Congestion management uses price-mechanisms and market-forces to prevent congestion. Various forms of congestion management exist and are applied to different problems. Congestion management is considered outside the scope of this thesis and is not discussed further on. Secondly, grid reinforcement is a viable solution. Nevertheless, this is a costly and time consuming process. The specifics of this solution are discussed in section 2.3. Lastly, grid scale energy storage is a promising option to relieve congestion [20]. This thesis focuses on grid scale energy storage, researching the viability of this solution. Other solutions are considered outside the scope of the research.

2.2 ENERGY STORAGE TECHNOLOGY

This section describes different energy storage technologies and provides a comparison between the different technologies. Firstly, energy storage in general is discussed, thereafter this section focuses on BESSs. The goal of this section is to gain understanding of different BESS technologies and to analyse the technical specification of this technologies. As, the selection of technology is crucial for the performance of a congestion relieving BESS.

The demand for energy storage solutions is growing, as energy storage systems can be paired with non-dispatchable sources of energy to prevent curtailment. The energy can be stored during periods of slumping demand and energy can be withdrawn from the storage system when generation is insufficient. There is a vast amount of different energy storage technologies with all their own benefits and challenges. Energy storage technologies can be divided in 5 main categories, namely: Electrochemical, Chemical, Electrical, Mechanical and Thermal. Each of this categories is used in different scenarios depending on the requirements of the given scenario. While comparing energy storage technologies different technical characteristics have to be taken into account such as the storage duration, efficiency, response time and levelised costs of energy [21]. Despite the vast variety of different energy storage technologies, this thesis focuses solely on electrochemical storage, namely batteries. An extensive research into and comparison of all different energy storage technologies is considered to be outside of the scope of this thesis. Furthermore, batteries are well suited as solution for congestion due to their high efficiency and fast response time.

2.2.1 Battery Energy Storage Systems

This section provides an overview of different BESS technologies. The technical specifications are reviewed and a comparison of the technologies is provided. The first part of this section compares all different technologies, subsequently a more thorough analysis of the most promising technology is executed.

A battery is a device that stores electrical energy in the form of chemical energy, hence electrochemical. The system that underpins the battery is called an electrochemical cell. A battery can be made up of one or multiple electrochemical cells, each electrochemical cell consists of two electrodes separated by an electrolyte. While discharging the battery an oxidation-reduction reaction happens in the cell and the free electrons flow through an external circuit. The negative or reducing electrode is called the anode, while the positive or oxidizing electrode is called the cathode. Different electrodes and electrolytes produce different chemical reactions that affect the batteries mechanics, how much energy it can store and its voltage.

Extensive research has been done into a vast amount of different technologies. Nevertheless, this thesis focuses on six different types of technologies. This six technologies are selected because they are seen as the leading electrochemical technologies for grid applications. This technologies are: Sodium-sulfur (NaS) batteries, Sodium-Nickel-Chloride (NaNiCl₂) Batteries, Lead-acid (Pb-Acid) batteries, Lithium-ion (Li-ion) batteries, Nickel-cadmium (Ni-Cd) batteries and Vanadium redox flow batteries (VRFB). Table 2.1 presents this six technologies with values for seven important characteristics for grid-scale batteries [22].

NaS batteries are found to be an interesting and emerging technology [23]. An important characteristic of NaS batteries is the operating temperature of 300°C [2]. NaS batteries have a high energy density and a decent round-trip efficiency between 80 and 90 percent [24],[25],[26]. This technology is already used for grid-scale applications and is considered to be a proven and commercialized technology. NaS batteries have high specific energy, which makes this technology suitable for high specific energy demanding applications [23].

The NaNiCl₂ battery was developed in 1985 by the Zeolite Battery Research Africa Project (Zebra), headed by Dr. Johan Coetzer at the Council for Scientific and Industrial Research in Pretoria, South Africa [27]. NaNiCl₂ batteries are considered a proven technology, but the technology is still commercialising [28]. The batteries have high round-trip efficiency [29] and a decent lifetime with up to 4500 cycles [30]. The batteries have low cost for energy and power [31], [28]. Furthermore, the specifications of this batteries make them suitable for stationary storage applications.

Pb-Acid batteries are characterized by low energy density and moderate round-trip efficiency [25], [32]. The main drawback is the low cycle life of this battery technology [2]. The cost of the battery cells is one of the main advantages of Pb-Acid batteries, costing only 54 - 400 USD/kWh. The low costs, low power and energy density in combination with the fast response time make Pb-Acid batteries particular suitable for stationary storage applications [33].

The Li-ion battery is a proven and fully commercialized technology. It is characterized by high energy and power density which makes the technology suitable for stationary and transportation applications[32]. There exist multiple types of lithium-ion batteries with their own benefits and challenges. The main challenge for most of the technologies are the high costs for energy and power capacity [34],[35], [36]. Later in this section an overview of the different Li-ion battery technologies is provided.

Ni-Cd batteries are characterized by their low energy density and moderate efficiency [37], [26]. One of the main issues of this technology is the use of the hazardous metal Cadmium, which causes a high environmental impact of this technology. The technology is commercialized for different applications, one of these is stationary energy storage [35].

Redox Flow batteries consist of two separate tanks, where two fluid electrolytes are contained. The two fluids are combined at two electrodes separated by a membrane, where the reduction-oxidation reaction occurs. The VRFB is the most mature of the different kinds of flow batteries. The technology is known to have a low power and energy density [38]. Furthermore, one of the biggest benefits of this technology is the fact that power and energy can be scaled independently [39]. This technology is mainly suitable for stationary applications.

	Energy Density (kWh/m ³)	Power Density (kW/m ²)	Round trip Efficiency (%)	Lifetime (Cycles)	Response Time (ms - s)	Energy Cost (dollar / kWh)	Power Cost (dollar/kW)
NaS	150 - 280 [24],[25]	150-300 [40]	80 - 90 [26]	4500 [2]	sec - 2 min [40],[35]	300 - 543 [40],[36]	380 - 3256 [36]
NaNiCl ₂	100 - 190 [41]	54 - 500 [32]	85 - 92.5 [26],[29]	2000-4500 [30]	<sec [22]	100 - 345 [31]	150 - 300 [28]
Pb-Acid	50 - 90 [25]	10 - 700 [40]	70 - 80 [32],[38]	<2500 [2]	1 - 10 ms [42],[40]	54 - 400 [36], [40]	200 - 651 [40], [43]
Li-ion	150 - 500 [25], [32]	50 - 5000+ [32]	85 - 95 [26], [41]	500 - 10000 [2]	20 ms - sec [40]	300 - 1200 [34]	900 - 4342 [35], [36]
Ni-Cd	15 - 150 [37], [44]	100 - 450 [25]	60 - 90 [26], [44]	2000-2500 [34]	20 ms - sec [40]	400 - 2400 [40]	500 - 1500 [40]
VRFB	10 - 70 [38]	0.5 - 34 [38]	60 - 85 [26]	>10000 [45]	sec - 10 min [35]	150 - 1085 [35], [36]	600 - 1628 [35], [36]

Table 2.1: Comparison of different battery technologies.

Various different Li-ion technologies exist, for example Lithium cobalt oxide-based, Lithium manganese oxide-based, Lithium nickel oxide-based, Lithium nickel cobalt aluminium oxide-based, Lithium nickel manganese cobalt oxide-based, Lithium titanate oxide-based and Lithium iron phosphate-based [2]. The main configurations that are being considered for grid-scale storage applications are: lithium Nickel Cobalt Aluminum Oxide-based (NCA), Lithium Nickel Manganese Cobalt Oxide-based (NMC) and Lithium Iron Phosphate-based (LFP). This is based on three key factors: high specific energy and power, durability, and material availability. Currently, NCA and NMC are used the most in grid-scale storage projects. Nevertheless, LFP cells, despite lower specific energy, are very promising for future implementation as the technology is relatively safe and has a very long durability [46].

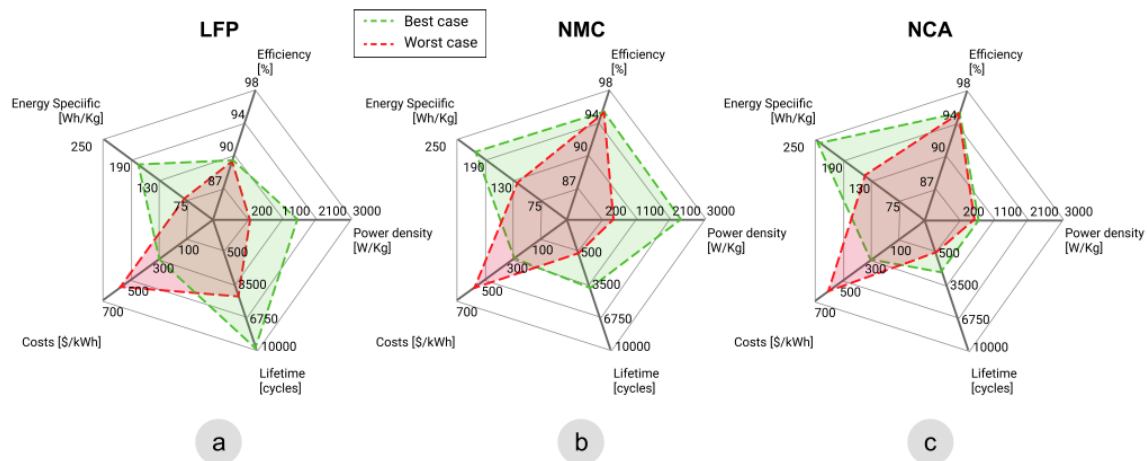


Figure 2.2: Comparison of power density, energy density, efficiency, costs and lifetime for the most popular Li-ion battery storage technologies for Grid applications: (a) Lithium Iron Phosphate, (b) Lithium Nickel Manganese Cobalt Oxide, (c) Lithium Nickel Cobalt Aluminum Oxide - author's elaboration from [2], [3] and [4]

Figure 2.2 presents the performances of (a) Lithium iron phosphate, (b) Lithium nickel manganese cobalt and (c) Lithium nickel aluminium cobalt batteries [2], [3] and [4]. From this electrochemical compositions, NMC offers the best overall performance. Its good performance, among other factors, led to NMC being the primary Li-ion technology for stationary storage and EVs [47], [2]. Comparing table 2.1 and figure 2.2 shows that the different lithium-ion technologies outperform the other technologies on multiple important parameters. Therefore, Lithium-ion batteries are the preferred choice for grid-scale storage applications. Therefore, this thesis focuses on this technology.

2.2.2 Battery Energy Storage System Setup

On its own, a Li-ion cell is not suitable for grid application. A extensive system of supportive technology is required. Therefore, this section aims to give an overview of the typical setup for grid-scale lithium-ion BESSs. Understanding the setup is crucial to design a BESS and to analyse the feasibility of a project.

Firstly, the core of the BESS consists of the battery packs, which are composed of multiple battery cells set up at the same voltage. This battery packs are responsible for the electrochemical storage of the energy. To form a functioning BESS from this battery packs, auxiliary technology is required. A schematic depiction of the main parts of a BESS is presented in figure 2.3. The Battery Management System (BMS) is required to monitor and maintain safe and optimal operations of each battery pack. The BMS collects measurement data from the battery cells. It is responsible for balancing the cells' voltage, protecting the cells from overloading and minimizing the temperature gradient to prevent uneven aging of the cells [48]. The BMS controls the charge and discharge rate, State of Charge (SoC) management and internal power electronic components. Furthermore, the BMS computes SoC and state of health data to feed this information to the Energy Management System (EMS). The EMS controls the storage system operations and protection. In addition to the data from the BMS, the EMS receives several external inputs, such as weather forecasts, energy market data, commands from DSOs, TSOs and aggregators. The decision algorithm embedded in the EMS uses this data to find P-Q set points of the storage system. These set point are digitally converted into the reference values for the DC-AC converter and send to the control board that drives the system [2].

Furthermore, a connection between the BESS and the AC grid is required. This connection is made through power electronics converters. The Power Conditioning System (PCS) accounts for a minor share of the total costs of lithium-ion based BESSs. Nevertheless, the decreasing price of battery packs results in a growing share in costs of the PCS [49]. To set up the voltage connection between the battery and the grid a transformer is the the most common solution. The AC voltage from the grid should be kept as high as possible to ensure a highly efficient DC-AC conversion. However, the maximum voltage is restricted by reliability issues, safety requirements, harmonic content, and P-Q capabilities set by the technical standards and national grid codes [50], [51], [2].

There is an increasing amount of companies that are moving towards a novel and integrated product where the battery, including all auxiliary systems is combined into one product. These products are designed to have the lowest external environmental impact [4].

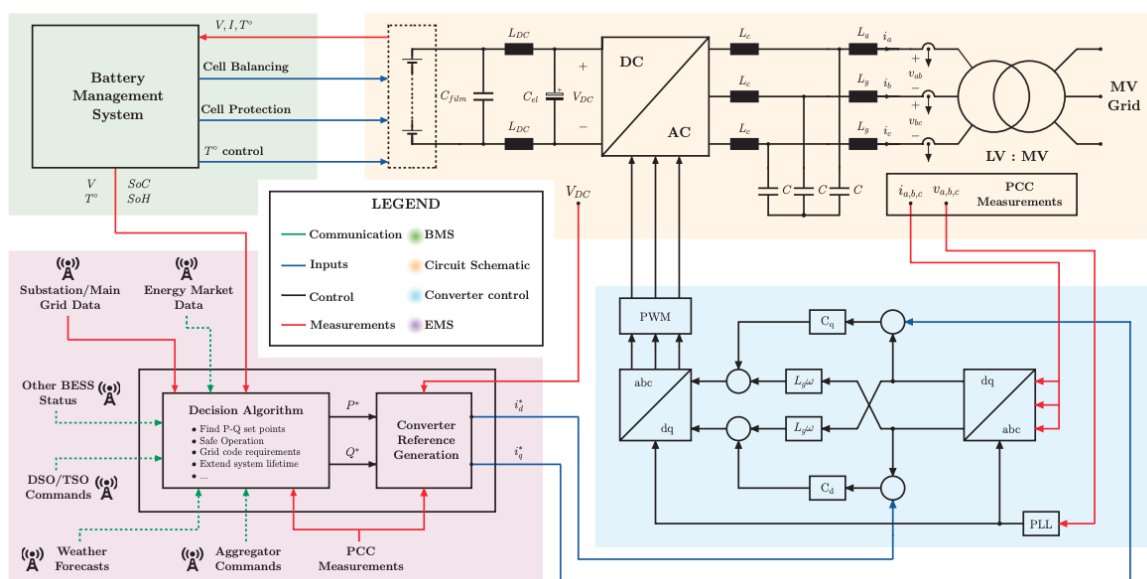


Figure 2.3: Battery Energy Storage System schematics and setup of the main components [2].

2.2.3 Battery Energy Storage System Lifetime Evaluation

This section describes the lifetime evaluation of Li-ion BESSs. The aim is to provide an overview of the degradation methods of Li-ion batteries and to provide a way to predict the degradation over time and the number of cycles. Battery degradation should be taken into account while determining the size and the charging/discharging strategy of a BESS, otherwise it is inevitable that the maximal potential of the battery is not matched.

With time and use, the storage capacity of Li-ion batteries decreases and the internal resistance increases. A wide range of degradation mechanisms exist, some occur simultaneously, others trigger further mechanisms [52]. Battery aging is enhanced by certain usage patterns and operating conditions. Nevertheless, the interplay between the different mechanisms is still not well understood [53]. There are three main external factors that influence the degradation of a battery: temperature, SoC and the load profile. The relative importance of each of these factors depends on, among others, the chemistry, form factor and historic use conditions [54]. Of this three factors the temperature is typically the most significant stress factor, deviations from the standard 25°C can lead to accelerated degradation. Operation on a higher SoC, as well as higher current operations, increase the likelihood of failure[55]. There are three tiers of detail to describe battery degradation. The most detailed tier is the degradation methods, these describe the physical and chemical changes that have occurred within the battery cell. These mechanisms are typically the hardest to observe. The next tier consists of degradation modes. Degradation modes are groups of degradation mechanisms, based on their overall impact on the cell's thermodynamic and kinetic behaviour. The last tier includes the observable effects of degradation, namely the capacity fade and the power fade of a battery. Capacity fade is the reduction of the usable capacity of the cell and power fade is a reduction of the deliverable power. These effects are the easiest to measure[54]. This thesis focuses on the observable effects of degradation because these are the most important during the design of a BESS. The more detailed tiers of degradation are considered outside the scope of this thesis.

Research has shown that besides the power cycling, the idling conditions of the cell contribute to the aging of Li-ion batteries [56]. The capacity fading effects are evaluated by the two empirical equations: 2.1 and 2.2. Equation 2.1 evaluates the calendar capacity fading C_{cal} , while equation 2.2 evaluates the cycling capacity fading C_{cyc} [57].

$$C_{cal}(25^{\circ}\text{C}) = 0.1723 \cdot e^{0.007388 \cdot \text{SoC}^*} \cdot t^{0.8} \quad (2.1)$$

$$C_{cyc}(25^{\circ}\text{C}) = 0.021 \cdot e^{-0.01943 \cdot \text{SoC}^{avg}} \cdot cd^{0.7612} \cdot nc^{0.5} \quad (2.2)$$

The capacity fading is a function of the average SoC of a cycle SoC_{avg} , the number of cycles nc of a certain cycle depth cd and the total time t that the battery is idling at a certain SoC level SoC^* . Both equation 2.1 and equation 2.2 describe the capacity fading of a battery at 25°C although the temperature is of large influence on the aging of a battery. Nevertheless, most connected batteries are equipped with an air-conditioning unit to keep the temperature at 25°C to ensure optimal performance. Furthermore, two empirical equations are used to evaluate the power fading of Li-ion batteries. Equation 2.3 describes calendar of fading of power, while equation 2.4 describes the power fading due to cycling patterns.

$$P_{cal} = \frac{0.000375 \cdot \text{SoC}^* + 0.1363}{0.155} \cdot 0.003738 \cdot e^{0.06778 \cdot T} \cdot t \quad (2.3)$$

$$P_{cyc} = \frac{1}{3} (5.78 \cdot 10^{-4} \cdot e^{0.03 \cdot T} + 1.22 \cdot 10^{-7} \cdot 2.918 \cdot 10^{-5} \cdot e^{0.08657 \cdot cd} \cdot nc^{(0.00434 \cdot T - 0.008 \cdot cd - 0.1504)}) \quad (2.4)$$

The equations for power fading are functions of the same variables as the equations for capacity fading, except in equation 2.3 and 2.4 the temperature T is included. The equations demonstrate

The high-voltage grid transmits electricity directly from the source to the regional distribution grids. The electricity is supplied to consumers through the distribution grid. In addition, the high-voltage grid supplies directly to large customers. The high-voltage grid and the distribution grids are connected at high-voltage substations or switching substations. At these nodes, transformers convert the high voltage to low voltage, suitable for the end-user. Figure 2.5 depicts how the voltage of the grid is gradually declining towards the end-users, through the use of different substations. The grid consists out of two types of building blocks, namely the different cables and the different substations. In the next part of this section this two building blocks are discussed.

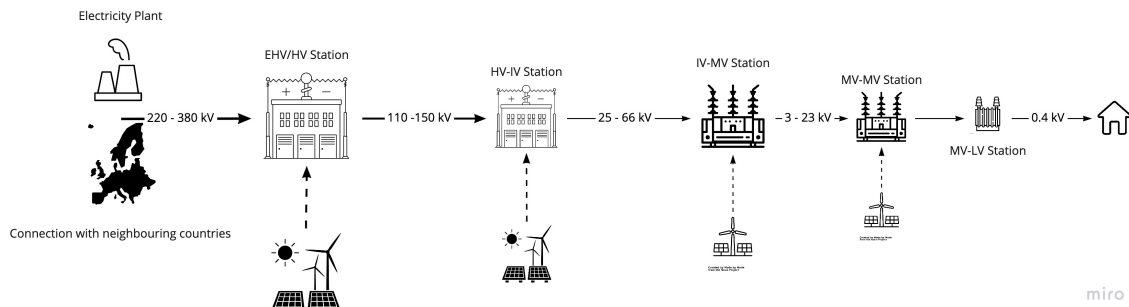


Figure 2.5: Layout of the electricity grid [5].

2.3.1 Electricity Cables

Electricity cables are divided in overhead and underground cables. The high-voltage overhead cables are generally not covered by insulation. The most commonly used conductor material is an aluminum alloy, made into several strands and possibly reinforced with steel strands. Historically, copper was frequently used for overhead cables but aluminum is lighter, yields only marginally reduced performances and has lower costs. Improvements in conductor materials and cable shapes are regularly designed to increase the capacity and to modernize transmission circuits. Nevertheless, it is outside of the scope of this thesis to research the cable configurations more in-depth. Furthermore, electric power can also be transmitted through underground power cables. Underground cables take up less right-of-way than overhead lines, have lower visibility, and are less affected by bad weather. However, costs of insulated cables and the excavation are much higher than overhead construction. Additionally, faults in underground transmission lines take longer to locate and repair. Table 2.2 presents an overview of some important numbers of the different cables used in the Netherlands. It is clear that higher Voltage cables lead to more expensive and more time consuming constructions. The numbers in the table are just an indication, depending on the location the numbers can differ.

Cable Type	Safety Area (m)	Construction Time	Costs (Euro/m)
Extra High Voltage (220 - 380 kV)	100	7 - 10 years	5,000 - 10,000
High Voltage (110 - 150 kV)	10	5 - 7 years	1,000 - 5,000
Intermediate Voltage (25 - 66 kV)	10	1 - 3 years	300 - 1,000
Medium Voltage (3 - 23 kV)	1 - 10	0.5 - 3 years	100 - 400
Low Voltage (0.4 kV)	1	0.5 - 1 year	70 - 150

Table 2.2: Overview of different electricity cables [5]

2.3.2 Electricity Substations

Electrical substations are the interface between the parts of the distribution grid and transmission grid with different voltages. Using transformers, these substations gradually step down the voltage in the transmission lines. Besides the transformers, substation are often equipped with a bus that splits off the current in multiple directions. Furthermore, circuit breakers are added, which

are used to interrupt any short-circuits or overload currents that may occur on the network. Additionally, switches which allow the isolation and direct control of certain parts of the transmission and distribution systems. Many substations include capacitors to smooth the voltage output. A more detailed description of substation is outside the scope of this thesis. Table 2.3 gives an overview of some important numbers of the different substations used in the Dutch transmission grid. Higher voltage substations are more expensive, are bigger in size and take longer to construct. Nevertheless, much less of these stations are needed than the ones for lower voltages. The numbers in the table are just an indication and depending on the location the numbers can differ.

Stations	Area (m ²)	Construction Time	Costs (10,000 Euro's)
Extra High Voltage/High Voltage (> 500 MVA)	40,000 - 100,000	7 - 10 years	> 10,000
High Voltage/Intermediate Voltage (100 - 300 MVA)	15,000 - 45,000	5 - 7 years	> 2,500
High Voltage/Medium Voltage (100 - 300 MVA)	15,000 - 40,000	5 - 7 years	> 2,500
Intermediate Voltage/Medium Voltage (20 - 100 MVA)	2,000 - 10,000	2.5 - 5 years	150 - 1000
Medium Voltage (10 - 40 MVA)	200 - 4,000	2.5 - 3 years	130 - 650
Medium Voltage/Low Voltage (0,2 - 1 MVA)	10 - 35	0.5 - 1 year	3.5 - 25

Table 2.3: Overview of the different substations[5]

2.4 ELECTRICITY MARKETS

Understanding the electricity market and its different aspects is necessary to design a model for a grid connected BESS. Therefore, this section aims to provide an overview of the different markets and market mechanisms.

2.4.1 Market Outline

Liberalisation and restructuring of the electricity sector dominates the energy policies in the European Union since mid-1990s. The goal of these policies is to design an efficient, competitive, and sustainable energy market across the European Union. The European introduced three electricity related directives (European Commission: 1996/92; 2003/54 and 2009/72) for the liberalization of the electricity markets in Europe [61]. One of the fundamental concepts of these directives is unbundling: the division of the market functions traditionally provided by a single utility into functionally independent parts. The degree of unbundling is decided by the policy makers. The Dutch policy makers chose the unbundling of ownership, which is the splitting of commercial activities from network operations. In this model, generation companies cannot acquire shares in network operators and similarly, network operators cannot hold shares of generation companies [62]. Furthermore, new regulations also introduced competition to the wholesale market through supplier selection. Starting with the large industrial consumers in 1998, the demand side of the Dutch market was fully liberalized by 2004 [63].

The directives of the European Commission actually aim to establish a single European Energy Market. This had led to the possibility to trade electricity on a pan-European auction. Nevertheless, at the moment different countries still have different market principles and rules. To narrow the scope of this thesis only the Dutch electricity market is discussed, which is seen as part of the European electricity trading scheme.

The different electricity markets can be divided based on settlement period and market principles. The Dutch market can be categorized in four groups: forward markets, day-ahead market, intra-day market and the balancing markets. Figure 2.6 gives a general overview of the different markets and their settlement periods. As a result of the technical characteristics of a BESS the wholesale markets and the balancing markets are interesting to participate in. Therefore, the section below discusses these markets in more detail.

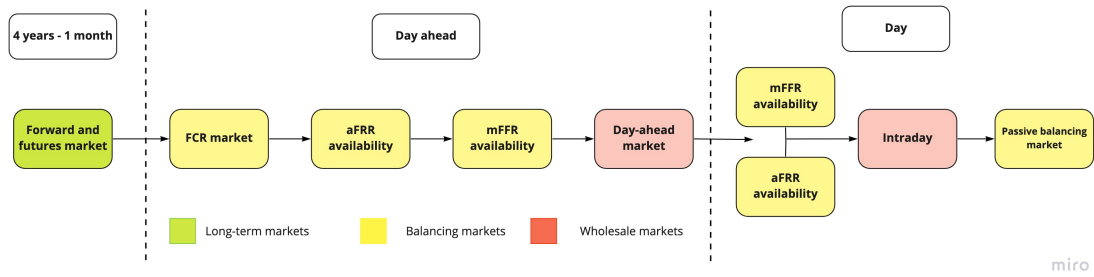


Figure 2.6: Layout of the electricity markets.

2.4.2 Day-Ahead Market

On the day-ahead market participants can buy and sell their electricity on a pan-European auction for the 24 hours of the next day. The electricity is auctioned in blocks of one hour. The market is cleared every day at 12:00 for the next day. Based on electricity demand predictions, suppliers provide demand curves to the exchange on a daily basis. Producers provide supply curves, which for example are based on expected generation of renewable energy sources. The settlement price is fixed at the intersection of offer and demand. The remuneration is based on Marginal pricing (also called pay-as-clear). Such method is a uniform pricing mechanism where all parties that are matched receive the same hourly clearing price. The marginal clearing price and the marginal clearing volume are determined for every hour of the day [64].

Unlike the long-term electricity market for bilateral trading between individual users, producers and third parties, the day-ahead market is only accessible for balance responsible parties. Balance responsible parties (BRPs) are responsible for maintaining supply and demand on the energy market within their own portfolio. BRPs are financially responsible for maintaining the balance between supply and demand of energy within their portfolio. The TSO bears the final responsibility to maintain stability and balance on the grid. Therefore, the TSO signs a contract with a BRP to establish the rights and obligations of both parties.

2.4.3 Intraday Market

After the clearing of the day-ahead market, the intraday market opens. This market has been developed to facilitate ongoing trade to avoid imbalances that could be derived from inaccurate predictions in the day-ahead market. In the Netherlands, the trading procedure of the intraday market, and thus the intraday price, is organized as continuous trading, procuring trades up to 5 minutes before delivery [65]. It is possible to trade electricity in intervals of a quarter, an hour or even five minutes. When a buy and sell bid are matched, a transaction is closed. Therefore, there is no single clearing price in this market. This price mechanism is called pay-as-bid [64].

The volumes traded on the Dutch intraday market have been increasing over the past years, i.e. 57% more volume was traded in 2019 than in 2018. Regarding the prices, 2016 and 2017 showed mostly higher intraday prices than day-ahead prices. However, this trend has shifted in 2018 and 2019. In those years, a higher day-ahead price than intraday price was experienced more frequent. Moreover, in 2019 the difference was even smaller than in 2018, with an increased number of hours with low price differences between the markets [66]. The increase in volatility of the intraday market is mainly caused by the higher share of weather dependant renewable energy sources in the Dutch energy portfolio. This causes a less predictable energy supply. Furthermore, like the day-ahead market, only BRPs can participate in the intraday market. so that the TSO is more secured against imbalances in the supply and demand.

2.4.4 Frequency Containment Reserve

The FCR market represents the primary frequency regulation control, which is automatically activated to ensure a constant ratio between frequency change and power change within a maximum time period of 30 seconds. The aim of the FCR is to stabilise frequency deviations in the interconnected European high-voltage grid, regardless of the cause and location of the disturbance. Primary control of the balancing services is procured internationally, all participating countries contribute their own share of FCR volume.

The FCR market is organised by the TSOs of the interconnected FCR scheduling areas. A daily auction in four hour blocks is held for the following day with a gate closure at 15:00. The market participant can make a bid by offering a certain amount of power capacity for the four hour blocks, with a minimal bid size of one MW. The volume can either be delivered by a single reserve providing unit or by a group of reserve providing units that combine their assets. Like the day-ahead market, the remuneration is based on marginal pricing. The market participant must be able to deliver 100% of the offered power capacity within 30 seconds. Furthermore, energy limited resources, such as BESSs, must be able to deliver 100% of its bid capacity for at least 15 minutes in case of a frequency deviation of 200 mHz [67].

2.4.5 Frequency Restoration Reserve

The TSOs activate the Frequency Restoration Reserve (FRR) consecutively to the FCR to gradually replace and therefore freeing up the original FCR capacity. The FRR is used to maintain real-time power and to balance the frequency after an event of power imbalance. FRR in the Netherlands is divided in two products: automatic Frequency Restoration Reserve (aFRR), which represents the secondary control reserves and the manual Frequency Restoration Reserve (mFRR), representing the tertiary control reserves. The way how the FCR, aFRR and mFRR are deployed is shown in figure 2.7 [6].

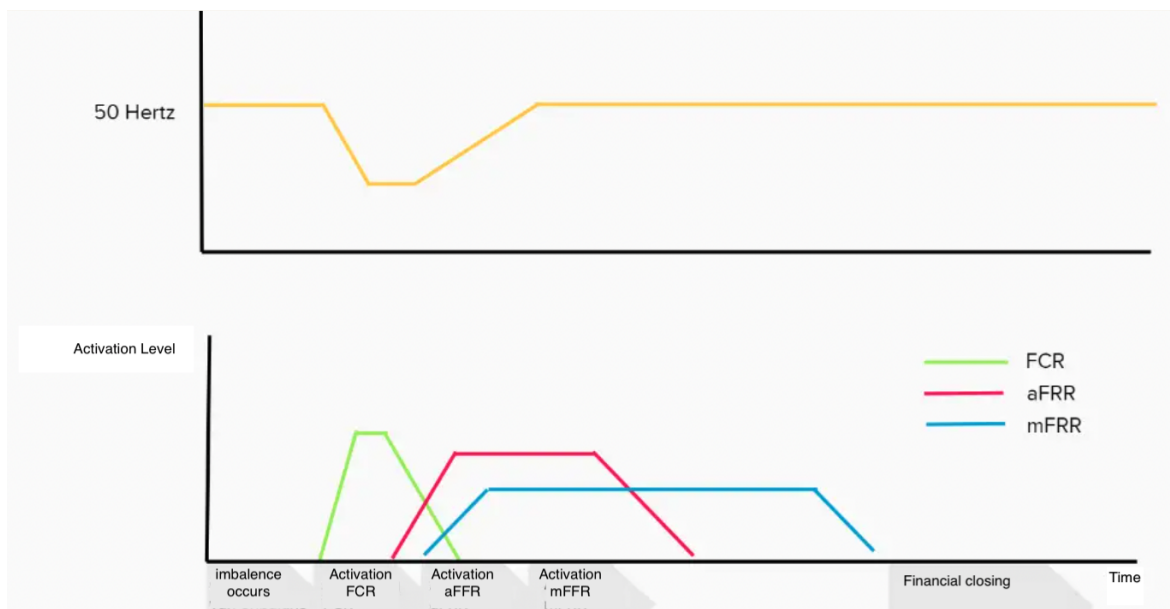


Figure 2.7: Overview of the balancing process [6].

All activated FRR (aFRR and mFRR) bids share the same imbalance price. The price is defined as the marginal price setting according to the merit order of all activated bids within an Imbalance Settlement Period (ISP). There are two forms of bidding, i.e. contracted capacity and free bidding, both forms compete with one another in each ISP. The remuneration is split into Activation (€/MWh) and Availability (€/MW). For aFRR contracted and voluntary bids have a minimal

capacity of one MW and it should be specified if this is for upward or downward regulation. Furthermore, the offered capacity requires an up- or down ramp rate of minimal seven percent of the bid volume per minute. The gate closure is the day before delivery and can be revised till 30 minutes before the ISP [68].

The mFRR is manually activated by the TSO in situations with long-lasting periods of significant system imbalance. These reserves are activated to free-up the previously activated aFRR, which then can become available for future imbalance disturbances. The mFRR is divided into the scheduled activated mFRRsa, which serves as the reserve power, and the direct activated mFRRda, representing the contracted emergency power. mFRRda participation is conducted through contracted capacity by daily auctions. The minimal contracted capacity is 20 MW and must be available for at least 60 minutes. mFRRsa participation occurs through voluntary bids and must prolong for at least one ISP. The remuneration for both form of mFRR is done according to the same principle as the aFRR [66].

2.4.6 Passive or Voluntary Balancing Market

The passive or voluntary balancing market (also referred to as the imbalance market) enables market parties to voluntarily contribute to maintaining the system balance based on actual imbalance prices. This market operates in parallel with Tennet activating contracted regulating power and/or imbalance netting through the International Grid Control Cooperation (IGCC).

To facilitate this market, TenneT publishes near real-time balancing information and settles imbalances for each BRP on a 15 minute basis. The market is settled based on the highest bid that has been activated during this ISP. The idea of this market is to provide an economic incentive for each BRP to assist in maintaining the system balance, even when they have to deviate from their own planned energy consumption or production. The amount of energy a BRP contributes is settled against the imbalance price for that ISP. The imbalance price is determined by the IGCC merit order at any moment. Nevertheless, Tennet is allowed to deviate from this price if a situation requires it, e.g. based on urgency [6].

The flexibility of a BESS can be exploited to economically optimise the energy consumption based on the imbalance price. The market provides opportunities for BESS owners to economically optimise power trades by accessing close to real time data on prices and volumes. The flexibility of a BESS provides the opportunity for energy arbitrage on the imbalance market. This could be a profitable strategy for BESS owners [66].

2.4.7 Potential of BESS on the Electricity Markets

There are different possibilities for BESS owners to generate revenue on the electricity markets. In this subsection a small overview of the possibilities is given.

Firstly, by using energy arbitrage profits can be made in the day-ahead, intra-day, and imbalance market. The idea is to buy the electricity when the prices are low, store the electricity and sell again when prices are high. A strong commitment dedicated to trade on the day-ahead market may not be the best possible option, as the price formations, on all the other markets (intraday and balancing), still have to occur for delivery in the same time frame. Therefore, the intraday market will likely be more attractive for a BESS owner. Nevertheless, it is still hard to create a profitable business case [69].

Additionally, the balancing markets are potentially profitable for BESS owners. Batteries, especially Li-ion batteries, are more feasible for FCR than FRR due to their limited energy capacity [66]. Having a high power to energy ratio is interesting for BESSs focused on FCR [70]. The fact that a battery can charge and discharge makes it well suited for this market application. Other earning opportunities can be pursued through the voluntary balancing market. As a result of the

growing share of RES in the energy generation, the amount of available power becomes harder to predict. This will lead to the necessity of more electricity trades closer to real time. Despite improving projections and forecasts, last-minute disruptions of the electricity generation may not be foreseen and catered for through intraday trades. Such unforeseen disruptions on a very short-term may result in scarcer, but high peak prices for voluntary balancing, from which a BESS could profit [71], [17].

Although, besides the balancing markets, other ancillary services for system operators are not within the scope of this thesis, securing an income from this kind of services is generally crucial for a BESS on the Dutch market. In this thesis it is considered that the BESS also relieves the congestion at a certain point in the grid, the BESS owner could be able to receive a compensation for this service through the TSO/DSO. Nevertheless, this compensation would be the result of a negotiation and is for this reason not included in the model.

In conclusion, the stacked participation of different markets seems to be the option with the highest potential. In this thesis, the combination of the FCR market and the voluntary balancing market is considered. The combinations of these two markets is seen as a combination with high potential in the literature [66].

2.5 OPTIMIZATION PROGRAMMING

This section describes the mathematical optimisation for the sizing of the BESS and the control strategy. There are many different approaches possible to tackle this problem. Nevertheless, this section focuses on the optimisation method chosen during this research.

In this thesis, the optimisation is done using (Mixed Integer) Linear Programming, as it is a widely used strategy for the optimisation of energy systems. Linear programming (LP) is a mathematical modeling technique in which a linear objective function is either maximised or minimised when subjected to various constraints. While Mixed Integer Linear Programming (MILP) has the same idea except some or all variables are restricted to be integers. The restriction of some variables to be integers is desirable for BESS optimisation, because some features like charging and discharging are binary. Moreover, binary variables can be used to approximate non-linear function as linear functions. Nevertheless, the addition of the integer variables leads to the necessity of more computational power to solve the problems [72].

The linearity of the objective function of (MI)LPs and the constraints ensures the convexity of the problem. As a result the solving of LPs can be done exceptionally efficient in most cases, while the results have a set of mathematical desirable features. The biggest problem is that non-linear functions can not be solved using (MI)LP, while multiple characteristics of BESS optimisation are described by non-linear functions. As described above, these functions have to be approximated with binary variables.

In conclusion, the application of linear programming can be highly computationally efficient. Nevertheless, when the formulations become more complex, especially for non-linear programming problems, this optimisation strategy faces difficulties in converging to an optimum solution. Therefore, it is important to create a model that is formulated as simple as possible [73].

3

LITERATURE REVIEW

In this chapter the existing literature on the topic of this research is reviewed. This chapter aims to provide an overview of the existing literature and to describe the knowledge gap that is being addressed in this thesis. Firstly, the topic of the thesis is summarized to clarify which literature is important. Secondly, the existing literature on the topic is presented. At last, the knowledge gap addressed in this thesis is discussed.

This thesis aims to investigate the feasibility of a profitable business case for a BESS, that relieves congestion on the Dutch electricity grid and utilizes the remaining capacity for market participation. For the market participation, the FCR and imbalance market are considered. This is investigated by designing multiple mathematical optimisation models using (MI)LP, using the models with real life case studies.

As BESS are seen as an important and promising technology for the energy transition, fast amount of research is done into all aspects that have to be considered for large scale BESS integration in the grid. First of all, as discussed in section 2.2.1, a variety of studies is done into different kinds of storage technologies in general [23], [74], [75], [22], [25], [32]. These papers compare the technical characteristics of the technologies. Nevertheless, their research is not focused on the implementation of the storage systems in the electricity grid. However, in [2], [42] and [34] a comprehensive review of BESSs in distribution grids is given. These papers provide an overview of different technologies and their feasibility in a distribution grid. Furthermore, the different possible applications of BESSs in distribution grids are discussed. [76] discusses these applications in the distribution grid as well, but solely focused on lithium-ion batteries. Furthermore, the application of grid-scale lithium-ion batteries in a distribution grid in the EMEA-region is discussed [46].

The technical aspects of different kinds of grid-scale energy storage systems have been thoroughly covered in the literature. Additionally, a general overview of the potential revenue streams of BESSs in the Netherlands is provided [66],[77].

Besides the general technical and financial overviews of BESSs, more in depth research has been done into the sizing and market participation of BESSs. For example, Byrne discusses the Energy Management System of grid scale energy storage and suggests a model to optimise market participation [78]. However, this is a general suggestion on how to construct a model instead of presenting a finished model and verifying it. Furthermore, [40] gives a general overview of different options to determine placement, sizing, and operations, while [73] gives an overview of different options to determine the BESS size. In both papers different options are proposed but neither presents a verified model. A more detailed model for the BESS sizing is given by [79]. In the paper, large-scale storage systems are introduced in a transmission network with high penetration of renewable energy sources. The size and location of the large-scale storage systems are optimised. The problem is mathematically formulated as the minimization of the production costs over a 24-hours-horizon. This optimises the overall network but does not optimise the size and operations for the BESS owner and does not optimise market participation.

Additionally, [80] presents a model to determine the utilisation of a BESS for congestion management. The model predicts day-ahead the amount of free capacity for other battery services. Nevertheless, the utilisation of this free capacity is not researched in the paper. Possibilities for the utilisation of the free capacity are discussed in [15]. The paper discusses optimisation of multi-scale energy market participation for different technologies. Nevertheless, the optimisation does

not consider congestion management and is not focused on BESSs and the Dutch energy market. The thesis of [4] models optimisation of the free capacity focused on the European energy market, specifically for the day-ahead market and the FCR market. Nevertheless, the paper does not consider the sizing of the BESS and variable congestion.

Furthermore, [16] proposes an optimal sizing and operations model for energy storage systems that are designed to remove congestion on the transmission grid. Two modelling philosophies are discussed, one which is focused on minimizing the overall cost of removing transmission congestion, and one which minimizes the investment cost of the storage facility. The models are focused on the Alberta energy system and all energy markets in the model act on the same timescale. Furthermore, this research does not consider battery degradation.

In conclusion, a vast amount of research has been done into the topic of this thesis. Nevertheless, this thesis fills a certain knowledge gap. Namely, by proposing a model that optimises the size and operations of a BESS that focuses on relieving congestion on the Dutch electricity grid while earning profit on the FCR and imbalance market. This model can be used to determine the feasibility of a business case of a congestion relieving BESS in the Dutch electricity grid.

4

MODEL FORMULATION

In this chapter, the models proposed to optimise the BESS size and market participation are described. The models aim to optimise the profit for the BESS-owner on the FCR and Imbalance market, while relieving congestion on the node of the grid where the BESS is placed. Four models are proposed, each with different optimisation principles. The first model optimizes for minimum investment with the assumption of perfect foresight and the second model optimises for maximum overall profit with the assumption of perfect foresight. The third model is similar to the first model, except uncertainties in load and market price forecasts are considered. The fourth and last model considers these uncertainties as well and introduces a risk factor. In the sections below each model is described and the methodology for creating the models is discussed.

4.1 METHODOLOGY

This section aims to describe the methodology of how the models are designed. In addition, this section presents the software used and outlines the way in which the models are formulated.

The optimisation models are written as a linear programming problem as described in subsection 2.5. To solve the linear programming problem a Python-based optimisation modeling language, called Pyomo, is used. Pyomo is an open-source optimisation modeling language with a diverse set of optimisation capabilities. Pyomo supports a wide range of problem types, but this thesis solely utilises linear programming and mixed integer linear programming. Pyomo does not come with a built in solver and therefore a supplementary solver has to be selected. Pyomo supports a large number of solvers, both open source and commercial. Pyomo can either invoke the solver directly or asynchronous with a solver manager. There are open-source solvers that are capable of solving the LP in the models, however in general the commercial solvers are more powerful and able to solve the LP and MILP problems faster with better performances. For this reason the Gurobi optimiser is selected. The Gurobi solver is free for academic use.

4.2 PERFECT FORESIGHT MODEL FORMULATIONS

As mentioned previously, two models based on perfect foresight are designed for this thesis. To construct this models a set of constraints and an objective function have to be formulated. In this section the sets of constraints and the objective function of the models are discussed.

4.2.1 Minimum Investment Model

The first model considered is the model for which minimum investment is required to relieve congestion. This model consists of two LP problems. The first LP problem finds the minimum possible investment to relieve the congestion, while the second finds the maximum revenue that is possible to acquire with this investment. For all optimisations, the technical characteristics of the chosen BESS are required. The influence of other parameters on the result may vary. For the minimum sizing of the BESS, the most important parameters are the load forecast on the cable or the substation, where congestion may occur, and the capacity of this asset. Based on these parameters

the first optimisation model finds the optimal sizing of the BESS for minimum investments. Thereafter, based on this sizing, the second LP problem investigates the maximum profit that could be generated through market participation. This is done by performing energy arbitrage on the imbalance market and by offering capacity on the FCR market. It is assumed that the bidding strategy of the BESS does not influence the market price, thus acting as price-taker.

Sizing Model

Before constructing the Linear programming model, the constraints must be formulated. For this problem almost all constraints are based on the technical characteristics of the BESS. The first two constraints prevent the charging or discharging power of the BESS from exceeding the power capacity of the BESS at any given time. These two constraint are given by equation 4.1a and 4.1b. Where P_t^{Chr} gives the charging power at time t , P_t^{Dis} gives the discharging power at time t and P^{BESS} gives the power capacity of the battery.

$$P_t^{\text{Chr}} \leq P^{\text{BESS}} \quad \forall t \in T \quad (4.1a)$$

$$P_t^{\text{Dis}} \leq P^{\text{BESS}} \quad \forall t \in T \quad (4.1b)$$

The next two constraints are based on the SoC of the battery. Equation 4.2a describes that the SoC of the battery at time t , SoC_t , is given by the SoC of the previous time-step, SoC_{t-1} , and the charging or discharging power of the battery at time t . In this model only the round-trip efficiency η of the battery is considered and for that reason the efficiency is only taken into account while charging. Constraint 4.2b demands that the SoC of the battery can not be less than 5 percent or more than 95 percent of the energy capacity of the battery, given by E^{BESS} . The two percentages are implemented because operating in this regions may cause harm to battery health.

$$\text{SoC}_t = \text{SoC}_{t-1} + \eta P_t^{\text{Chr}} \Delta t - P_t^{\text{Dis}} \Delta t \quad \forall t \in T \quad (4.2a)$$

$$0.05 \cdot E^{\text{BESS}} \leq \text{SoC}_t \leq 0.95 \cdot E^{\text{BESS}} \quad \forall t \in T \quad (4.2b)$$

Furthermore, a constraint is formulated such that the congestion is relieved at any time and no extra congestion is caused by the BESS. Constraint 4.3 dictates that the load on the cable/substation, P_t^{load} , plus the charging power or minus the discharging power is never greater than the capacity of the cable/substation, P^{Capacity} . This causes the relief of congestion and prevents the BESS from causing congestion. The left side of the formula is absolute, as the capacity can not be surpassed in the opposite direction.

$$|P_t^{\text{load}} + P_t^{\text{Chr}} - P_t^{\text{Dis}}| \leq P^{\text{Capacity}} \quad \forall t \in T \quad (4.3)$$

The last constraint is established to ensure that the number of cycles, nc , of the BESS is smaller than the maximum number of cycles, $maxcycles$, chosen in the time-range of the simulation. This is to prevent high cycling aging effects on the batteries. Constraint 4.4a keeps the number of cycles below the maximum number of cycles and equation 4.4b describes how the number of cycles is calculated. The number of cycles is calculated by dividing the charging energy by the energy capacity.

$$nc \leq maxcycles \quad (4.4a)$$

$$nc = \sum_{t=1}^T P_t^{\text{Dis}} \cdot \Delta t / E^{\text{BESS}} \quad \forall t \in T \quad (4.4b)$$

To complete the LP problem, the constraints are combined with the objective function. The objective function is formulated as the minimisation of the capital costs of power per MW, Capex^P , multiplied with the power capacity combined with the capital costs of energy per MWh, Capex^E , multiplied by the energy capacity. As a result, equation 4.5 describes the LP problem of the first model.

$$\begin{aligned}
& \underset{p^{\text{BESS}}, E^{\text{BESS}}}{\text{minimise}} && \text{Capex}^P p^{\text{BESS}} + \text{Capex}^E E^{\text{BESS}} \\
& \text{subject to} && p_t^{\text{Chr}} \leq p^{\text{BESS}} \quad \forall t \in T \\
& && p_t^{\text{Dis}} \leq p^{\text{BESS}} \quad \forall t \in T \\
& && \text{SoC}_t = \text{SoC}_{t-1} + \eta p_t^{\text{Chr}} \Delta t - p_t^{\text{Dis}} \Delta t \quad \forall t \in T \\
& && 0.05 \cdot E^{\text{BESS}} \leq \text{SoC}_t \leq 0.95 \cdot E^{\text{BESS}} \quad \forall t \in T \\
& && |p_t^{\text{load}} + p_t^{\text{Chr}} - p_t^{\text{Dis}}| \leq p^{\text{Capacity}} \quad \forall t \in T \\
& && \text{nc} \leq \text{maxcycles}
\end{aligned} \tag{4.5}$$

Revenue Model

The second part of the model has the objective to maximise the revenue for the battery size proposed by the first part of the model, while still relieving the congestion. This results in the necessity of extra parameters to build this model, i.e. the market prices. As the BESS operates on both the FCR and Imbalance market, the market prices of these two markets are considered. The introduction of these two markets also leads to a new set of constraints, although some constraints stay the same. Constraints 4.2a, 4.2b, 4.3 and 4.4a are the same as in the sizing model. Constraint 4.2a stays the same because of the assumption that the power offered on the FCR market does not effect the SoC. Furthermore, new constraints are introduced, such as the constraints for the power capacity. Due to the introduction of the FCR market and the dynamics of this market, the power capacity offered on this market cannot be traded and cannot exceed the power capacity of the battery. This is described by constraints 4.6a and 4.6b, where p_z^{FCR} describes the power offered on the FCR market. Additionally, the FCR market works with bids that have 4 hour increments while the imbalance market has quarterly hour increments. Therefore, an additional time series is introduced: z . The two time series are coupled using the time discretisation scheme proposed by [15].

$$p_t^{\text{Chr}} + p_z^{\text{FCR}} \leq p^{\text{BESS}} \quad \forall t, z \in T, Z \tag{4.6a}$$

$$p_t^{\text{Dis}} + p_z^{\text{FCR}} \leq p^{\text{BESS}} \quad \forall t, z \in T, Z \tag{4.6b}$$

Furthermore, two extra constraints are added to prevent simultaneous charging and discharging. These constraints are essential, because unlike a real battery, the model is able to preform this behaviour. In equation 4.7a and 4.7b a binary variable, d_t , is added to prevent simultaneous charging and discharging.

$$p_t^{\text{Chr}} \leq p^{\text{BESS}} \cdot d_t \quad \forall t \in T \tag{4.7a}$$

$$p_t^{\text{Dis}} \leq p^{\text{BESS}} \cdot (1 - d_t) \quad \forall t \in T \tag{4.7b}$$

The introduction of the FCR market demands constraints to obey this market's regulations. The rules of the FCR market state that batteries have to be able to deliver the capacity that is offered for a minimum time of 15 minutes. This means that the SoC has to provide this power during the whole time the capacity is offered on the FCR market. This is described in constraints 4.8a and 4.8b, where Δt is 15 minutes.

$$p_z^{\text{FCR}} \cdot \Delta t \leq 0.95 \cdot E^{\text{BESS}} - \text{SoC}_t \quad \forall t, z \in T, Z \tag{4.8a}$$

$$p_z^{\text{FCR}} \cdot \Delta t \leq \text{SoC}_t - 0.05 \cdot E^{\text{BESS}} \quad \forall t, z \in T, Z \tag{4.8b}$$

It should be considered that the rules of the FCR market dictate that bids can only be done in increments of one MW. Therefore, the variable p_z^{FCR} should be defined as an integer in the Pyomo model. The objective function of this model is formulated to maximise the sum of the profits on the FCR and imbalance market, thus the volume traded on the market multiplied by the prices,

λ_t^{Imb} and λ_z^{FCR} . To guide the decision-making process a ramp cost is added to the equation. This adds a cost for the cycling of the battery, and thus reduces the number of cycles. This value is important to prevent fast degradation and excessive cycling. The value of the ramp cost, C_{ramp} , represents the marginal cost of the system, considered as the operation and management cost, which is based on the average of one cycle per day considered as full energy throughput. The value is 8 €/MWh, which means that at least an 8 €/MWh price spread is needed in the imbalance market for the BESS to be profitable. For the FCR market the same strategy is applied, except the value of the ramp cost, C_{rampFCR} , is defined differently. C_{rampFCR} represents the ratio of the sum of the cost of the battery system and the Balance of Plants on the max operative hours in a year [69], [72].

$$\begin{aligned}
& \underset{p_t^{\text{Chr}}, p_t^{\text{Dis}}, p_z^{\text{FCR}}}{\text{maximise}} && \sum_{t=1}^T (\lambda_t^{\text{Imb}} - C_{\text{ramp}}) p_t^{\text{Dis}} \Delta t - \sum_{t=1}^T (\lambda_t^{\text{Imb}} + C_{\text{ramp}}) p_t^{\text{Chr}} + \sum_{z=1}^Z (\lambda_z^{\text{FCR}} - C_{\text{rampFCR}}) \cdot p_z^{\text{FCR}} \\
& \text{subject to} && p_t^{\text{Chr}} + p_z^{\text{FCR}} \leq p^{\text{BESS}} \quad \forall t, z \in T, Z \\
& && p_t^{\text{Dis}} + p_z^{\text{FCR}} \leq p^{\text{BESS}} \quad \forall t, z \in T, Z \\
& && p_t^{\text{Chr}} \leq p^{\text{BESS}} \cdot d_t \quad \forall t \in T \\
& && p_t^{\text{Dis}} \leq p^{\text{BESS}} \cdot (1 - d_t) \quad \forall t \in T \\
& && \text{SoC}_t = \text{SoC}_{t-1} + \eta p_t^{\text{Chr}} \Delta t - p_t^{\text{Dis}} \Delta t \quad \forall t \in T \\
& && 0.05 \cdot E^{\text{BESS}} \leq \text{SoC}_t \leq 0.95 \cdot E^{\text{BESS}} \quad \forall t \in T \\
& && |p_t^{\text{load}} + p_t^{\text{Chr}} - p_t^{\text{Dis}}| \leq p^{\text{Capacity}} \quad \forall t \in T \\
& && p_z^{\text{FCR}} \cdot \Delta t \leq 0.95 \cdot E^{\text{BESS}} - \text{SoC}_t \quad \forall t, z \in T, Z \\
& && p_z^{\text{FCR}} \cdot \Delta t \leq \text{SoC}_t - 0.05 \cdot E^{\text{BESS}} \quad \forall t, z \in T, Z
\end{aligned} \tag{4.9}$$

4.2.2 Maximum Profit Model

The second model aims to maximise the profit of the BESS over its lifetime. This means that the size can differ from the minimum size defined by the first model. The extra revenue generated by a bigger system could outweigh the extra costs of the bigger system. This model could be viewed as a combination of the two separate LPs of the minimum investment model. It combines the important parameters of the two models in a new model with a new objective. This means that all the constraints are the same as in equation 4.14. The objective function is a combination of the objective function of 4.5 and 4.14. Thus, equation 4.10 is the model to maximise the profit generated by the BESS over its lifetime.

$$\begin{aligned}
& \underset{p_t^{\text{Chr}}, p_t^{\text{Dis}}, p_z^{\text{FCR}}, p^{\text{BESS}}, E^{\text{BESS}}}{\text{maximise}} && \zeta - \theta \\
& \text{subject to} && \theta = \text{Capex}^P p^{\text{BESS}} + \text{Capex}^E E^{\text{BESS}} \\
& && \zeta = \sum_{t=1}^T (\lambda_t^{\text{Imb}} - C_{\text{ramp}}) p_t^{\text{Dis}} \Delta t - \sum_{t=1}^T (\lambda_t^{\text{Imb}} + C_{\text{ramp}}) p_t^{\text{Chr}} \\
& && + \sum_{z=1}^Z (\lambda_z^{\text{FCR}} - C_{\text{rampFCR}}) p_z^{\text{FCR}} \quad \forall t, z \in T, Z \\
& && p_t^{\text{Chr}} + p_z^{\text{FCR}} \leq p^{\text{BESS}} \quad \forall t, z \in T, Z \\
& && p_t^{\text{Dis}} + p_z^{\text{FCR}} \leq p^{\text{BESS}} \quad \forall t, z \in T, Z \\
& && p_t^{\text{Chr}} \leq p^{\text{BESS}} \cdot d_t \quad \forall t \in T \\
& && p_t^{\text{Dis}} \leq p^{\text{BESS}} \cdot (1 - d_t) \quad \forall t \in T \\
& && \text{SoC}_t = \text{SoC}_{t-1} + \eta p_t^{\text{Chr}} \Delta t - p_t^{\text{Dis}} \Delta t \quad \forall t \in T \\
& && 0.05 \cdot E^{\text{BESS}} \leq \text{SoC}_t \leq 0.95 \cdot E^{\text{BESS}} \quad \forall t \in T \\
& && |p_t^{\text{load}} + p_t^{\text{Chr}} - p_t^{\text{Dis}}| \leq p^{\text{Capacity}} \quad \forall t \in T \\
& && p_z^{\text{FCR}} \cdot \Delta t \leq 0.95 \cdot E^{\text{BESS}} - \text{SoC}_t \quad \forall t, z \in T, Z \\
& && p_z^{\text{FCR}} \cdot \Delta t \leq \text{SoC}_t - 0.05 \cdot E^{\text{BESS}} \quad \forall t, z \in T, Z
\end{aligned} \tag{4.10}$$

4.3 UNCERTAINTY BASED OPTIMISATION MODELS

The models presented in the previous sections of this chapter are based on perfect predictions of the load and the energy prices. This section describes for both models a variant where uncertainties in the predictions are taken into account. The uncertainties are considered by incorporating stochastic modeling and in the last model a risk factor is added using the Conditional Value at Risk (CVaR).

4.3.1 Uncertainty Based Programming Methodology

This section describes the methodology used to account for the uncertainties in load and market predictions. The models are again written as MILP problems and solved using the Gurobi solver with Pyomo. The model where the minimum investment is considered, uses stochastic modeling and for the model where the maximum profit is considered the CVaR is used.

Stochastic modeling is often used in the literature to simulate uncertainties in energy systems [8], [81], [82]. A stochastic model develops a mathematical model to derive the possible outcomes of a problem using random input variables. The focus is on the probability of different scenarios. In this thesis, the probability of different market and load scenarios is considered. The advantage of stochastic modeling is that the uncertainties are taken into account, which makes the model

more realistic. The downside of stochastic models is that they can be computationally complex to perform, and may require a more in-depth statistical and computational ability than some of the simpler deterministic models. The CVaR method is used to account for the risk of investment considering uncertain prediction, where the total profit is maximised. The CVaR method is a well know method to consider the risk of investment and has been discussed extensively in literature [16], [83], [84]. CVaR is the extended risk measure of Value At Risk (VaR) that quantifies the average loss or profit over a specified period of time of unlikely scenarios beyond the confidence level. CVaR is defined as the expected loss exceeding an upper percentile of a loss function; the upper percentile is known as the VaR [85]. CVaR is incorporated into the model to limit the risk of high losses for the BESS owner, as it has low computational burden, well-established mathematical properties.

4.3.2 Uncertainty Minimum Investment Model

Firstly, the stochastic model for the minimum investment model is described. For the stochastic model, again two LP problems are constructed. The models are constructed fairly similar to their deterministic counterpart, except in this case the uncertainties of the market prices and load data are taken into account.

Uncertainty Sizing Model

In the first part of the minimum investment model the only uncertainty is presented by the load predictions. To consider the uncertainty of the load profiles on a certain part of the grid, first of all the probability of different scenarios should be considered. In this thesis, it is assumed that the load prediction at every moment in time has a normal distribution with the predicted value as the mean of the distribution. The purpose of this model is to relieve congestion with a 99 % probability. Figure 4.1 shows a normal distribution with the different probabilities for different standard deviations, σ .

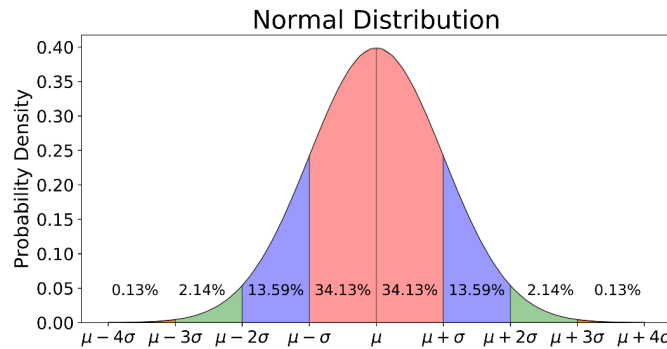


Figure 4.1: Normal Distribution [7].

From figure 4.1 it can be concluded that 99 % of the probability density function is located left of the mean plus 2.33 standard deviations. This leads to the first constraint of the model, i.e. equation 4.11.

$$|p_t^{\text{load}} + p_t^{\text{Chr}} - p_t^{\text{Dis}}| \leq p^{\text{Capacity}} - 2.33\sigma \quad \forall t \in T \quad (4.11)$$

The equation is very similar to equation 4.3, only the 2.33σ is added to account for the uncertainty of the load prediction. As explained above, there is only one percent probability that the load at a given moment is higher than the predicted value plus 2.33 standard deviation. Therefore, the 2.33 standard deviation is deducted from the capacity. The value for the standard deviation is determined by the accuracy of the predictions and has to be determined based on the data that is used.

In reality the standard deviation would increase for predictions further in the future, as these are less accurate. Nevertheless, in this model it is assumed that the standard deviation stays the same over the entire period, as an in-depth research on uncertainties is outside the scope of this thesis. The rest of the model stays the same as 4.5. The model for the BESS sizing is described by equation 4.12.

$$\begin{aligned}
& \underset{P^{\text{BESS}}, E^{\text{BESS}}}{\text{minimise}} && \text{Capex}^P P^{\text{BESS}} + \text{Capex}^E E^{\text{BESS}} \\
& \text{subject to} && P_t^{\text{Chr}} \leq P^{\text{BESS}} \quad \forall t \in T \\
& && P_t^{\text{Dis}} \leq P^{\text{BESS}} \quad \forall t \in T \\
& && \text{SoC}_t = \text{SoC}_{t-1} + \eta P_t^{\text{Chr}} \Delta t - P_t^{\text{Dis}} \Delta t \quad \forall t \in T \\
& && 0.05 \cdot E^{\text{BESS}} \leq \text{SoC}_t \leq 0.95 \cdot E^{\text{BESS}} \quad \forall t \in T \\
& && |P_t^{\text{load}} + P_t^{\text{Chr}} - P_t^{\text{Dis}}| \leq P^{\text{Capacity}} - 2.33\sigma \quad \forall t \in T \\
& && \text{nc} \leq \text{maxcycles}
\end{aligned} \tag{4.12}$$

Uncertainty Based Revenue Model

The second part of the uncertainty minimum investment model aims to maximise profit. The size determined by the uncertainty sizing model is used. Besides the uncertainty in the load, in this model the uncertainty in the market prices is considered. A different approach considering the uncertainties has to be chosen, as the values of the market prices and the load influence the strategy. Working with a threshold does not work for this model. Therefore, in this model, different scenarios for the load, the FCR price and the imbalance price are combined to create a stochastic model. As mentioned previously, it is assumed that the uncertainty of the load expectations follow a normal distribution. To determine the scenarios and their probability to occur, the probability density function has to be converted to discrete levels [8]. The way this is accomplished is described in figure 4.2.

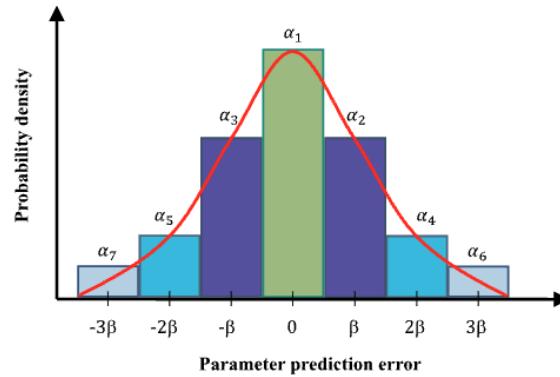


Figure 4.2: Conversion of probability density function to discrete levels [8].

The scenarios of the FCR and imbalance prices can be generated using the same strategy as the one used for the load data. It is important to choose realistic standard deviations for the predictions and to choose a realistic probability density function based on the data that is used. The stochastic model for the maximum revenue is based on the models described in [86], [8], [81]. The model is fairly similar to the deterministic model for the maximum revenue, except for the fact that in this case, different scenarios are introduced. This leads to the objective function presented by equations 4.13a and 4.13b.

$$\underset{P_{f,i,l,t}^{\text{Chr}}, P_{f,i,l,t}^{\text{Dis}}, P_{f,i,l,t}^{\text{FCR}}}{\text{maximise}} \sum_{f \in F} \sum_{i \in I} \sum_{l \in L} \zeta_f \zeta_i \zeta_l (\zeta_{f,i,l}) \quad \forall f, i, l \in F, I, L \quad (4.13a)$$

$$\zeta_{f,i,l} = \sum_{t=1}^T ((\lambda_{f,i,l,t}^{\text{Imb}} - C_{\text{ramp}}) P_{f,i,l,t}^{\text{Dis}} \Delta t) - \sum_{t=1}^T ((\lambda_{f,i,l,t}^{\text{Imb}} + C_{\text{ramp}}) P_{f,i,l,t}^{\text{Chr}} \Delta t) \quad (4.13b)$$

$$+ \sum_{z=1}^Z ((\lambda_{f,i,l,t,z}^{\text{FCR}} - C_{\text{rampFCR}}) P_{f,i,l,t,z}^{\text{FCR}}) \quad \forall f, i, l, t, z \in F, I, L, T, Z$$

Equations 4.13a and 4.13b take the average of all possible scenarios considering their probability to occur. The different scenarios for the FCR prices are described by the subscript f , for the imbalance prices by the subscript i and for the load by the subscript l . The probability of occurrence is given by respectively, ζ_f , ζ_i and ζ_l . The rest of the model is structured in the same way, where the deterministic model is applied for every possible scenario occurring. This leads to the stochastic MILP problem described by equations 4.14.

$$\underset{P_{f,i,l,t}^{\text{Chr}}, P_{f,i,l,t}^{\text{Dis}}, P_{f,i,l,t}^{\text{FCR}}}{\text{maximise}} \sum_{f \in F} \sum_{i \in I} \sum_{l \in L} \zeta_f \zeta_i \zeta_l (\zeta_{f,i,l})$$

subject to

$$\zeta_{f,i,l} = \sum_{t=1}^T ((\lambda_{f,i,l,t}^{\text{Imb}} - C_{\text{ramp}}) P_{f,i,l,t}^{\text{Dis}} \Delta t) - \sum_{t=1}^T ((\lambda_{f,i,l,t}^{\text{Imb}} + C_{\text{ramp}}) P_{f,i,l,t}^{\text{Chr}} \Delta t)$$

$$+ \sum_{z=1}^Z ((\lambda_{f,i,l,t,z}^{\text{FCR}} - C_{\text{rampFCR}}) P_{f,i,l,t,z}^{\text{FCR}}) \quad \forall f, i, l, t, z \in F, I, L, T, Z$$

$$P_{f,i,l,t}^{\text{Chr}} + P_{f,i,l,t}^{\text{FCR}} \leq P^{\text{BESS}} \quad \forall f, i, l, t, z \in F, I, L, T, Z$$

$$P_{f,i,l,t}^{\text{Dis}} + P_{f,i,l,t}^{\text{FCR}} \leq P^{\text{BESS}} \quad \forall f, i, l, t, z \in F, I, L, T, Z$$

$$P_{f,i,l,t}^{\text{Chr}} \leq P^{\text{BESS}} \cdot d_{f,i,l,t} \quad \forall f, i, l, t \in F, I, L, T$$

$$P_{f,i,l,t}^{\text{Dis}} \leq P^{\text{BESS}} \cdot (1 - d_{f,i,l,t}) \quad \forall f, i, l, t \in F, I, L, T$$

$$\text{SoC}_{f,i,l,t} = \text{SoC}_{f,i,l,t-1} + \eta P_{f,i,l,t}^{\text{Chr}} \Delta t - P_{f,i,l,t}^{\text{Dis}} \Delta t \quad \forall f, i, l, t \in F, I, L, T$$

$$0.05 \cdot E^{\text{BESS}} \leq \text{SoC}_{f,i,l,t} \leq 0.95 \cdot E^{\text{BESS}} \quad \forall f, i, l, t \in F, I, L, T$$

$$|P_{f,i,l,t}^{\text{load}} + P_{f,i,l,t}^{\text{Chr}} - P_{f,i,l,t}^{\text{Dis}}| \leq P^{\text{Capacity}} \quad \forall f, i, l, t \in F, I, L, T$$

$$P_{f,i,l,t,z}^{\text{FCR}} \cdot \Delta t \leq 0.95 \cdot E^{\text{BESS}} - \text{SoC}_{f,i,l,t} \quad \forall f, i, l, t, z \in F, I, L, T, Z$$

$$P_{f,i,l,t,z}^{\text{FCR}} \cdot \Delta t \leq \text{SoC}_{f,i,l,t} - 0.05 \cdot E^{\text{BESS}} \quad \forall f, i, l, t, z \in F, I, L, T, Z$$
(4.14)

4.3.3 Risk-Based Maximum Profit Model

As mentioned previously, for the model where the profit for the BESS owner is maximised, the CVaR is incorporated to introduce a risk factor. By incorporating the CVAR method to the formulation, the objective of this model changes to that of minimising the CVaR for the BESS owner while maximising the profit of the BESS. The weight of these two objectives is determined by the risk factor. The model will also provide a measure on how much of the BESSs cost will likely be carried by the BESS owner, given the uncertainties in generating additional revenues from the market by sharing the excess capacity [16]. In the same way as in the maximum revenue model, different scenarios are created for the market prices and for the load profile. As described in the methodology part of this section, CVaR is defined as the upper percentile of a loss function, where the upper percentile is known as VaR. The loss function is described by equations 4.15a, 4.15b and 4.15c [87].

$$f(\theta, \zeta) = \theta - \zeta_{f,i,l} = \pi_{f,i,l} \quad \forall f,i,l \in F,I,L \quad (4.15a)$$

$$\theta = \text{Capex}^P P^{\text{BESS}} + \text{Capex}^E E^{\text{BESS}} \quad (4.15b)$$

$$\begin{aligned} \zeta_{f,i,l} = & \sum_{t=1}^T ((\lambda_{f,i,l,t}^{\text{Imb}} - C_{\text{ramp}}) P_{f,i,l,t}^{\text{Dis}} \Delta t) - \sum_{t=1}^T ((\lambda_{f,i,l,t}^{\text{Imb}} + C_{\text{ramp}}) P_{f,i,l,t}^{\text{Chr}} \Delta t) \\ & + \sum_{z=1}^Z ((\lambda_{f,i,l,z}^{\text{FCR}} - C_{\text{rampFCR}}) \cdot P_{f,i,l,z}^{\text{FCR}}) \quad \forall f,i,l,t,z \in F,I,L,T,Z \end{aligned} \quad (4.15c)$$

Equation 4.15a describes the loss function, equation 4.15b describes the investment costs and equation 4.15c describes the profit obtained through the two electricity markets. This equation also introduces the uncertainty, as the market and load conditions are uncertain. The loss function is a random variable with cumulative distribution introduced by ζ , for each value of the θ . As provided in [87], the mathematical definition of VaR and CVaR is characterised and discretised, which is described by equation 4.16.

$$F(\pi_{f,i,l}, \epsilon) = \epsilon + (1 - \beta)^{-1} \sum_{f \in F} \sum_{i \in I} \sum_{l \in L} \zeta_f \zeta_i \zeta_l [\pi_{f,i,l} - \epsilon]^+ \quad (4.16)$$

In equation 4.16, ϵ is the value at risk threshold and β represents the confidence interval defined by the BESS owner. The minimisation of equation 4.16 is equivalent to the minimisation of $CVaR^\beta$, while obtaining a near optimal value for VaR^β . The term $[\pi_{f,i,l} - \epsilon]^+$ introduces a non-linearity to the model. Nevertheless, by introducing a non negative auxiliary variable $z_{f,i,l}$ this non-linearity can be avoided. This is described by equation 4.17.

$$z_{f,i,l} \geq \pi_{f,i,l} - \epsilon \quad (4.17)$$

This methodology leads to the risk-based optimisation model described by 4.18, where the risk and the cost for the BESS owner are minimised. The rest of the model consists of the same constraints as presented by LP problem 4.14.

$$\begin{aligned} \text{minimise} \quad & \pi_{f,i,l}^{\text{FCR}}, \epsilon \quad \omega \left(\sum_{f \in F} \sum_{i \in I} \sum_{l \in L} \zeta_f \zeta_i \zeta_l (\pi_{f,i,l}) \right) + (1 - \omega) (\epsilon + (1 - \beta)^{-1} \sum_{f \in F} \sum_{i \in I} \sum_{l \in L} \zeta_f \zeta_i \zeta_l z_{f,i,l}) \\ \text{subject to} \quad & z_{f,i,l} \geq \pi_{f,i,l} - \epsilon \quad \forall f,i,l \in F,I,L \\ & \pi_{f,i,l} = \theta - \zeta_{f,i,l} \quad \forall f,i,l \in F,I,L \\ & \theta = \text{Capex}^P P^{\text{BESS}} + \text{Capex}^E E^{\text{BESS}} \\ & \zeta_{f,i,l} = \sum_{t=1}^T ((\lambda_{f,i,l,t}^{\text{Imb}} - C_{\text{ramp}}) P_{f,i,l,t}^{\text{Dis}} \Delta t) - \sum_{t=1}^T ((\lambda_{f,i,l,t}^{\text{Imb}} + C_{\text{ramp}}) P_{f,i,l,t}^{\text{Chr}} \Delta t) \\ & \quad + \sum_{z=1}^Z ((\lambda_{f,i,l,z}^{\text{FCR}} - C_{\text{rampFCR}}) \cdot P_{f,i,l,z}^{\text{FCR}}) \quad \forall f,i,l,t,z \in F,I,L,T,Z \\ & P_{f,i,l,t}^{\text{Chr}} + P_{f,i,l,z}^{\text{FCR}} \leq P^{\text{BESS}} \quad \forall f,i,l,t,z \in F,I,L,T,Z \\ & P_{f,i,l,t}^{\text{Dis}} + P_{f,i,l,z}^{\text{FCR}} \leq P^{\text{BESS}} \quad \forall f,i,l,t,z \in F,I,L,T,Z \\ & P_{f,i,l,t}^{\text{Chr}} \leq P^{\text{BESS}} \cdot d_{f,i,l,t} \quad \forall f,i,l,t \in F,I,L,T \\ & P_{f,i,l,t}^{\text{Dis}} \leq P^{\text{BESS}} \cdot (1 - d_{f,i,l,t}) \quad \forall f,i,l,t \in F,I,L,T \\ & \text{SoC}_{f,i,l,t} = \text{SoC}_{f,i,l,t-1} + \eta P_{f,i,l,t}^{\text{Chr}} \Delta t - P_{f,i,l,t}^{\text{Dis}} \Delta t \quad \forall f,i,l,t \in F,I,L,T \\ & 0.05 \cdot E^{\text{BESS}} \leq \text{SoC}_{f,i,l,t} \leq 0.95 \cdot E^{\text{BESS}} \quad \forall f,i,l,t \in F,I,L,T \\ & |P_{f,i,l,t}^{\text{load}} + P_{f,i,l,t}^{\text{Chr}} - P_{f,i,l,t}^{\text{Dis}}| \leq P^{\text{Capacity}} \quad \forall f,i,l,t \in F,I,L,T \\ & P_{f,i,l,z}^{\text{FCR}} \cdot \Delta t \leq 0.95 \cdot E^{\text{BESS}} - \text{SoC}_{f,i,l,t} \quad \forall f,i,l,t,z \in F,I,L,T,Z \\ & P_{f,i,l,z}^{\text{FCR}} \cdot \Delta t \leq \text{SoC}_{f,i,l,t} - 0.05 \cdot E^{\text{BESS}} \quad \forall f,i,l,t,z \in F,I,L,T,Z \end{aligned} \quad (4.18)$$

4.3.4 Lifetime Evaluation

In this section, the methodology to evaluate the lifetime of the BESS is discussed. The lifetime of the BESS is determined by the rate of degradation. In section 2.2.3, the necessary background information on battery degradation is provided.

To determine the lifetime of BESSs in this thesis, only the capacity fading is studied. As mentioned in section 2.2.3, the capacity fading is determined by the cycling conditions and the idling conditions of the battery. The equations to determine these two mechanisms are given by equations 2.1 and 2.2, and are repeated below.

$$C_{\text{cal}}(25^{\circ}\text{C}) = 0.1723 \cdot e^{0.007388 \cdot \text{SoC}^*} \cdot t^{0.8} \quad (4.19)$$

$$C_{\text{cyc}}(25^{\circ}\text{C}) = 0.021 \cdot e^{-0.01943 \cdot \text{SoC}^{\text{avg}}} \cdot cd^{0.7612} \cdot nc^{0.5} \quad (4.20)$$

In this thesis, it is assumed that the battery is kept at a constant temperature of 25°C , thus the effects of temperature fluctuations are neglected. The calendar capacity fading is determined by the time the battery is inactive at a certain SoC. These values are determined directly from the SoC profile of the battery.

The cycling capacity fading of the battery is determined by a series of cycles, each with different cd and SoC^{avg} . The operation of the BESSs in this thesis is highly irregular, as the operation is subject to a large number of variables. Therefore, identifying directly the number of cycles, the cd and SoC^{avg} is difficult to derive from the SoC profiles. To overcome this difficulty, the rainflow counting algorithm [88] is adopted. This model is widely used in fatigue studies and has been applied to battery cycle analysis in [89] and [90]. Nevertheless, in this thesis it is assumed that the operations on the FCR market do not effect the SoC, thus these operations are not taken into account for the capacity fading.

The rainflow counting algorithm takes the battery's SoC profile as input, identifies all the local extreme points, and then determines the cd and SoC^{avg} based on the local extrema sequence [91]. Figure 4.3 gives an example of the rainflow counting algorithm. In this figure the local extreme points are extracted from the SoC profile and are used to determine either full or half cycles. For example, 2 till 2' represent a full cycle, while 7 till 9 represent two half cycles with different cycle depths [92].

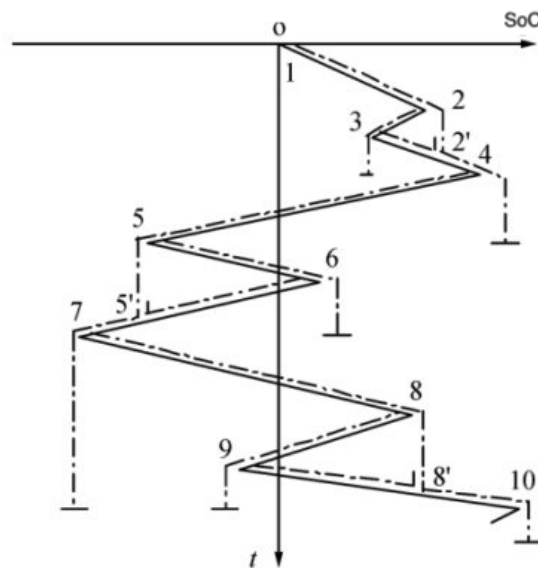


Figure 4.3: Example of the rainflow counting algorithm.

The determination of rainflow cycles in this thesis is done in Python using the rainflow 3.1.1 implementation from PyPi [93].

To determine the lifetime of the BESS, the two capacity fading mechanisms are combined to determine the total capacity fading. As mentioned in 2.2.3, it is assumed that the BESS has reached its end of life when 20% of the capacity has faded. Therefore, this point is used to estimate the total lifetime of the BESS.

5

CASE STUDIES AND DATA ANALYSIS

In this chapter, the case studies and the market data are discussed. The three selected case studies are based on data provided by the Dutch DSO Liander. The case studies are based on nodes in the Dutch electricity grid where structural congestion is expected. In all cases the BESS will be placed behind the node to relieve the congestion. It is assumed that in all cases Liander would be able to connect the BESS no matter the power capacity of the BESS, although in reality this is not always the case, as the connection capacity is limited. Furthermore, it is assumed that either the BESS owner is a BRP or has a contract with a BRP, thus can participate in both markets. The electricity price data is provided by the company EnAppSys.

Firstly, the three case studies are discussed and the available data is evaluated. Thereafter, the preparation of this data for the uncertainty models is discussed. At last, electricity market data is presented.

5.0.1 Overview of the Case Studies

In this section the different case studies are discussed. An overview of the congestion problem in the different areas is provided and important background information is discussed. Two of the three case studies are located in Amsterdam and the other one is located on the Dutch island Terschelling. The two case studies in Amsterdam are about the areas IJpolder and Westhaven. In the two case studies located in Amsterdam, the congestion is expected to occur at an electricity substation. For the case study on Terschelling, the congestion is expected to occur at an electricity cable. The case studies are selected in collaboration with Giga Storage and Liander. Structural congestion is a big problem for Liander and therefore Liander seeks new solutions for this problem. The three case studies are based on locations where Liander has done extensive analysis of the grid and discovered the risk of structural congestion. These locations are selected, as Liander is willing to run pilots for the usage of BESSs to relieve the congestion in this areas.

IJpolder

DSO Liander did an extensive analysis of the grid and discovered a risk of structural congestion at the grid area below the IJpolder transmission station. The area covered by the grid below station IJpolder is presented in figure 5.1.

The congestion occurs as the demand for electricity is increasing and the capacity of the grid is not sufficient for this increase. This leads to problems for the people who are currently connected in the IJpolder area and it results in the fact that new connections must be postponed. Liander plans to expand the transmission station at the end of 2026. Nevertheless, due to the increasing demand for electricity it is important to investigate other solutions. For that reason, this thesis investigates the possibility of a congestion relieving BESS in this area. Liander has provided an expected quarter-hourly load profile for 2026. This load profile is based on historic data and the expected load profiles of new connections. The fast amount of historic load data at the transmission station and the relatively predictable load profiles of new connections makes the estimation of the load relatively accurate [9]. Figure 5.2 shows the load profile for 2026 and the capacity, 35 MW, of the station, as this will be the capacity of the station till at least 2026.

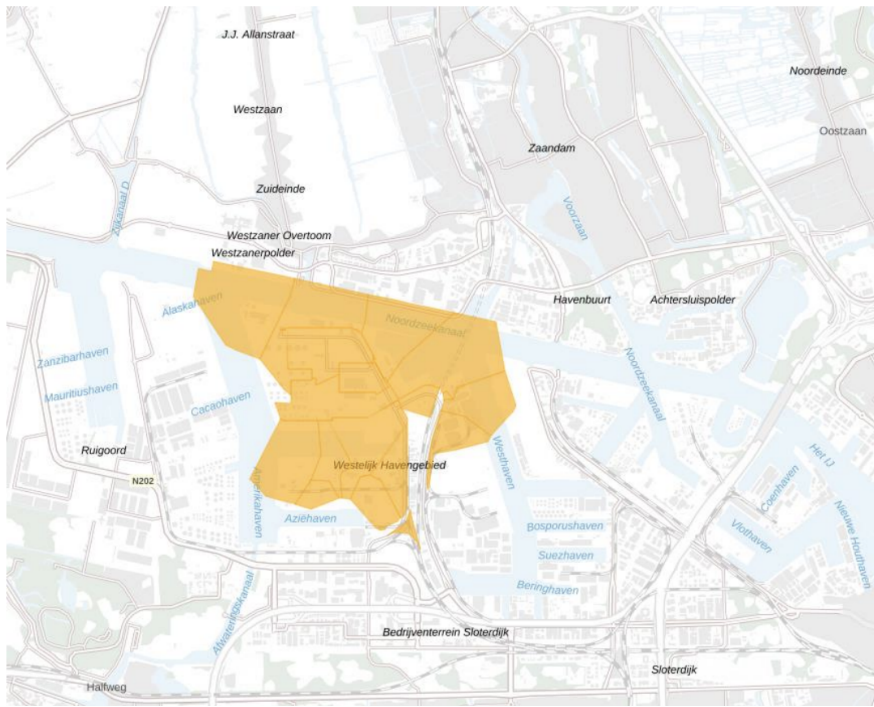


Figure 5.1: Overview of the IJpolder congestion area [9].

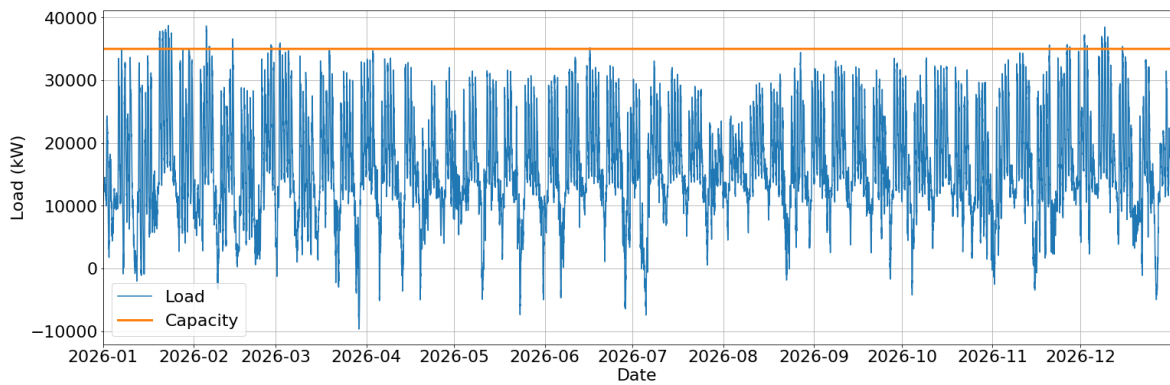


Figure 5.2: Load and capacity on IJpolder transmission station.

From figure 5.2, it can be concluded that the congestion mainly occurs during the winter and that the congestion problem is relatively small in this area. Furthermore, from the load profile and the capacity, the important numbers to describe the situation can be determined. Table 5.1 gives an overview of these important numbers. The negative number at minimum load indicates that electricity is flowing from the IJpolder area back into the grid. These numbers are important to determine the minimum size of the BESS.

Maximum Load	38.72 MW
Minimum Load	- 9.66 MW
Maximum consecutive time of congestion	7.5 hours
Total time of congestion	76 hours
Total energy that could not be transported	102.73 MWh

Table 5.1: Important numbers at station IJpolder in 2026.

Terschelling

The next case study is about the Dutch island Terschelling. Terschelling is a relatively small island with a population of 4960 and no big industry. This leads to a lower energy demand than in the IJpolder area. Nevertheless, structural congestion is expected to occur on the island. Figure 5.3 gives an overview of the congested area.



Figure 5.3: Overview of the Terschelling congestion area [10].

The fact that Terschelling is an island makes this case interesting, as the reinforcement of the grid is more complicated and expensive. In contrary to the other case studies, the station is not the problem on Terschelling, it is the cable to the island. There are plans to expand the cable. Nevertheless, this is a time consuming process. Therefore, Liander provided the expected quarter-hourly load data for the island in 2030 and the capacity of 8 MW [10]. The load profile is depicted in figure 5.4. Again the most congestion occurs in the winter. Furthermore, the difference between winter and summer is bigger than in the IJpolder region. The exact reason for this cannot be determined with certainty, as the composition of the energy portfolios in both areas is not public. Obvious reasons are: more year-round industry at IJpolder and a higher share of solar generation on Terschelling.

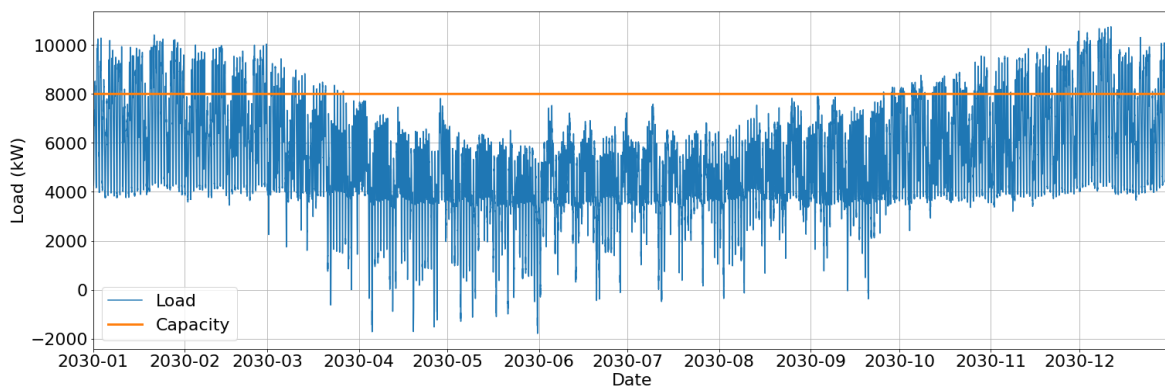


Figure 5.4: Load and capacity on Terschelling transmission station.

Figure 5.4 shows that during the winter of 2030 congestion is expected regularly. Congestion occurs more regular than in the IJpolder case. Nevertheless, the absolute power capacity shortage is lower. Again the load profile and capacity is used to determine the important numbers to describe the situation. These numbers are posted in table 5.1. The table shows that the congestion in Terschelling is more severe than in the IJpolder area, as the total energy that could not be transported is higher.

Maximum Load	10.75
Minimum Load	- 1.79 MW
Maximum consecutive time of congestion	14 hours
Total time of congestion	1074.25 hours
Total energy that could not be transported	959.52 MWh

Table 5.2: Important numbers at station Terschelling in 2030.

Westhaven

The last case study is about the transmission station Westhaven. Like IJpolder, Westhaven is an area in Amsterdam and as all case studies the station is managed by DSO Liander. Liander concluded from a grid analysis that in this area structural congestion will occur. This leads to the same problem as the other case studies. There are plans to expand the capacity in 2026. Nevertheless, it is interesting to investigate what the role of a BESS could be [11]. The area is depicted in figure 5.5.

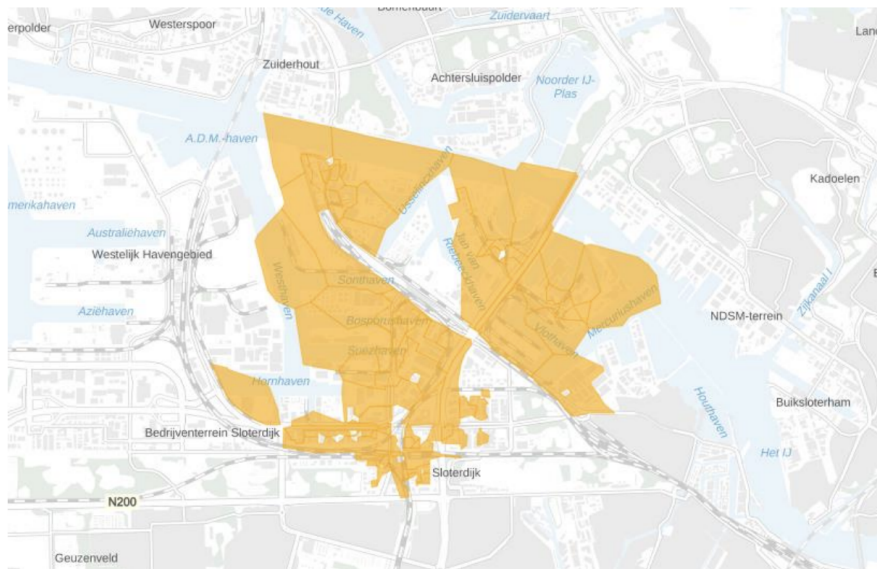


Figure 5.5: Overview of the Westhaven congestion area [11].

The area depicted in figure 5.5, is located in Amsterdam, there is a lot of industry located and the demand for energy is high. The predicted congestion problems prevent new connections in the area, which is holding back the economic growth of the area. The load profile of the Westhaven area is predicted and the prediction for 2026 together with the capacity of 66 MW is depicted in figure 5.6.

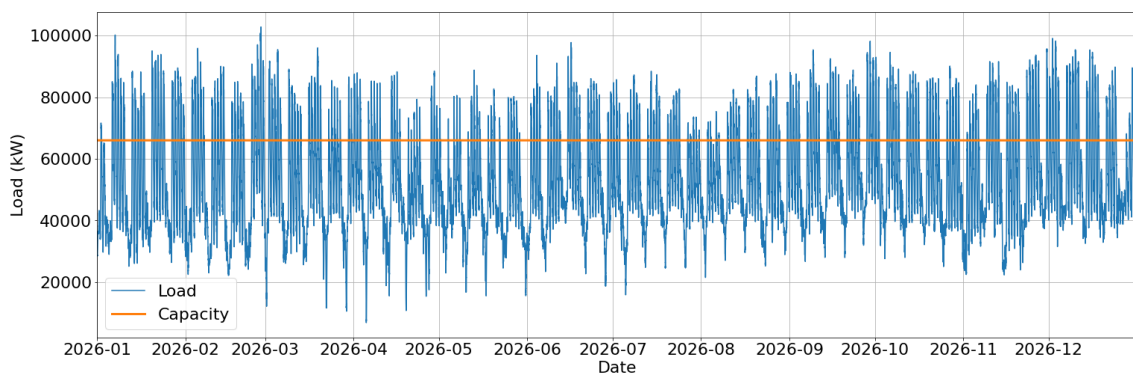


Figure 5.6: Load and capacity on Westhaven transmission station.

Figure 5.6 shows that congestion occurs frequently throughout the whole year and that the energy demand is higher than for the IJpolder and Terschelling case studies. There is some seasonality, though less than at Terschelling. In the same way as the other case studies, the load profile provides the important numbers. These numbers are collected in table 5.3.

Maximum Load	102.76 MW
Minimum Load	- 6.87 MW
Maximum consecutive time of congestion	14.25 hours
Total time of congestion	2265.25 hours
Total energy that could not be transported	26322.44 MWh

Table 5.3: Important numbers at station Westhaven in 2026.

5.0.2 Uncertain Load Data

Section 4.3.2 mentioned that the uncertainty scenarios of the load are created through discretisation of the normal distribution. The development of more scenarios leads to a more accurate model. Nevertheless, more scenarios cause the necessity of more computational power. Therefore, there is chosen to work with three scenarios in this thesis.

To choose the scenarios, the standard deviation of the normal distribution must be determined first. The standard deviation of the distribution is based on the standard error of the forecast. The standard error is calculated by comparing estimated data with real data and using equation 5.1.

$$\sigma_{forecast} = \sqrt{\frac{\sum_{n=1}^N (y - y')^2}{N}} \quad (5.1)$$

Where $\sigma_{forecast}$ is the standard error, y is the real data y' is the predicted data and N the number of data point. Nevertheless, this data is not available for the case studies. Therefore, a value for the standard deviation of the probability density function must be assumed, though this is far from the ideal situation. It is important to make a reasonable assumption. Long term load data forecast is discussed in the literature [94]. Nevertheless, Liander has the advantage that everyone with a connection bigger than 1000 kW has to present their planned demand or supply for the next ten years. Furthermore, Entsoe reports that through the GARPUR project a novel methodology to forecast load profile is developed. The results of this model are supported by a 95% confidence interval [95]. Therefore, in this thesis the standard deviation of the load forecast is assumed to be 200 kW. In the ideal situation this value was calculated for every case study independently and the horizon of the forecast should be taken into account. Nevertheless, as this is an estimation the standard deviation is assumed to be constant for all case studies. The first scenario is the value as this given by the forecast, this is assumed to be the mean of the normal distribution. The other two scenarios are given by the mean plus and minus two sigma.

The probability of the scenarios occurring is calculated as figure 4.2 proposes, this leads to the probabilities presented in table 5.4.

Value	Probability
Forecast - 2σ	0.15865
Forecast	0.6827
Forecast + 2σ	0.15865

Table 5.4: Probability of the different load scenarios

5.0.3 Electricity Price Data

The electricity price data is provided by EnAppSys. EnAppSys is a company specialised in the energy markets and have their own energy data platform. They use classical and machine learning algorithms to predict future energy prices. They provided three scenarios for the FCR prices and the imbalance prices. One high scenario, one medium and one low, for this thesis it is assumed that in each point of time every scenario has an equal probability of occurring. Nevertheless, for the models where perfect foresight is assumed the medium scenario is chosen. The average prices of all scenarios per day of the two relevant years are presented in figures 5.7 and 5.8. As expected, the Imbalance prices are higher on average and the delta of the prices is bigger.

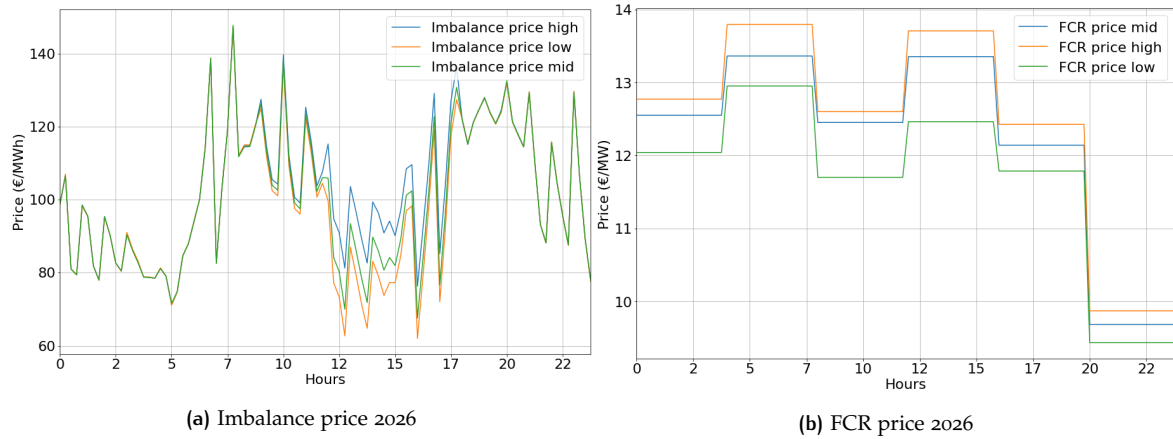


Figure 5.7: Average market prices for the high, medium and low scenarios in 2026.

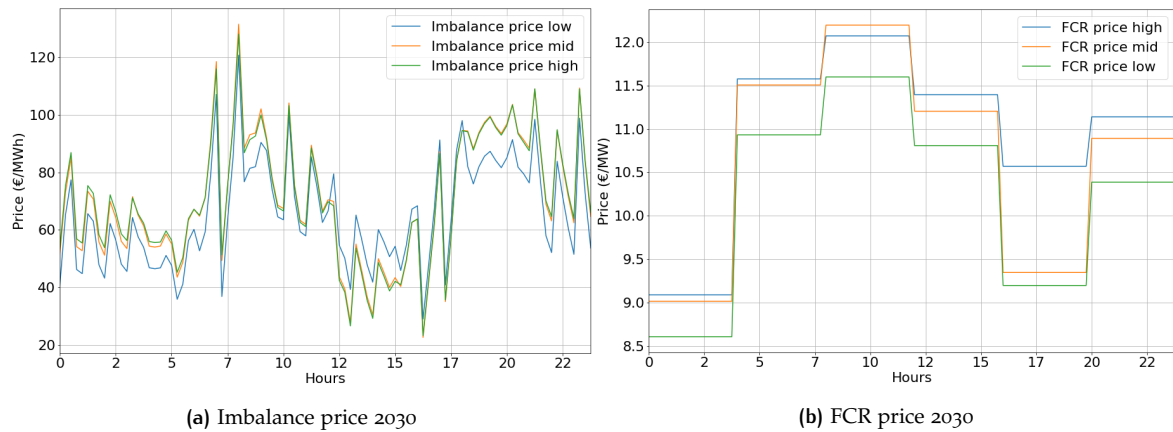


Figure 5.8: Average market prices for the high, medium and low scenarios in 2030.

6 | RESULTS

In this section the results of the models for the different case studies are provided. The results of every model are discussed and a comparison of the results is provided. The results of the different case studies are presented and compared. Furthermore, the results of the lifetime evaluations are presented. Firstly, the models, where perfect foresight is assumed, are discussed. Thereafter, the models with the consideration of uncertainty are discussed.

To determine the results, the parameters of the models must be determined. The parameters that should be determined are the round-trip efficiency of the BESS, the capital cost per kW for the power capacity and the capital cost per kWh for the energy capacity. Table 2.1 provides the data for this parameters. The round trip efficiency of the BESS is assumed to be 90%. According the last report of the NREL, the capital costs of a battery are approximately 350€ per kWh [96]. Furthermore, The cost for the Power Electronics Converter and the Balance of the Plant is assumed to be 150€ per kW. This value is derived according to the solar utility market, since utility scale Voltage source converters of photovoltaic generators are similar systems to the ones used in BESS [56]. These numbers are used for all models and case studies. However, based on the project at hand, one can easily calculate these values in a more precise matter. These parameters are summarized in table 6.1.

Parameter	Value
Round trip efficiency	90%
Capital cost of Power	€150 per kW
Capital cost of Energy	€350 per kWh

Table 6.1: Parameters used in the different models.

6.1 MINIMUM INVESTMENT MODEL

The minimum investment model determines the minimum power and energy capacity to solve congestion. The minimum sizes are determined by solving the LP problem presented by LP 4.5. The inputs are the load data of the corresponding case study and the parameters presented in table 6.1.

Thereafter, these sizes are used to determine the maximum profit that can be achieved through market operations, while still relieving the congestion. The profit is determined by solving the LP problem proposed by 4.14. The load profile, the FCR prices and Imbalance prices are used as input for the model in combination with the parameters presented in table 6.1.

The two models lead to the results presented in table 6.2. The load profiles presented in chapter 5 provide information on the severity of the congestion. This severity has an observable influence on the BESS sizing. Westhaven requires the biggest BESS to solve the congestion. For the IJpolder case study less congestion occurs, leading to a smaller BESS. The size of the BESS for the Terschelling case study has a value between the two others, so does the severity of congestion. Furthermore, it is clear that larger BESSs generate more profit through market operations, as the traded volumes are larger. Nevertheless, if the capital costs and the total profits are compared between the different case studies it becomes clear that IJpolder has a higher return on investment compared to the other two case studies.

	Ijpolder	Terschelling	Westhaven
Storage Power Capacity (MW)	3.725	3.709	36.763
Storage Energy Capacity (MWh)	16.180	27.573	525.209
Capital costs BESS (Million €)	6.22	10.21	189.34
Profit from imbalance market (Million €)	0.738	0.826	4.285
Profit from FCR market (Million €)	0.130	0.082	1.548
Total profit of market operation (Million €)	0.868	0.907	5.833
Number of Cycles	461	294	126

Table 6.2: The results from the minimum investment model

In figures 6.1, 6.2, and 6.3, the output of the BESS for the different case studies for the first month of the year is presented. In the graphs positive values indicate charging of the battery and negative values indicate discharging. The charging and discharging on the imbalance market happens with a higher frequency than the participation on the FCR market. Figure 6.3 shows that the output on the FCR market is often maximised to be 25 MW as it is assumed that only indivisible bids are allowed on the FCR market.

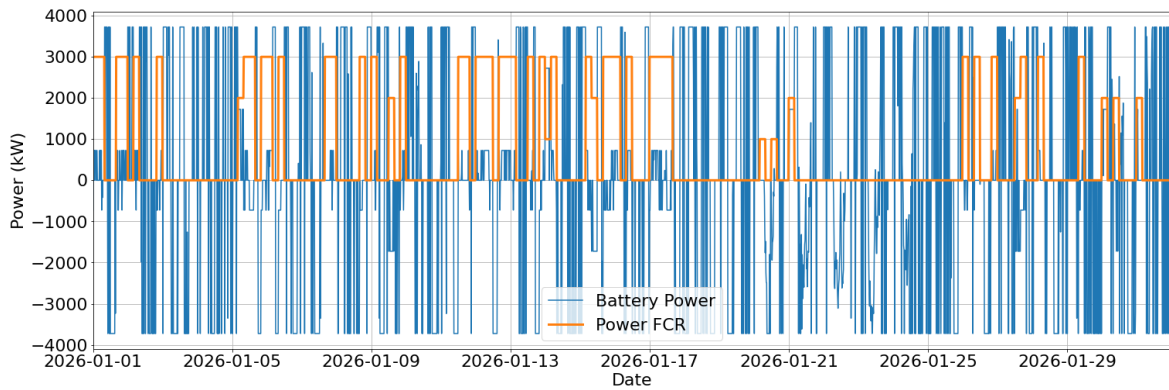


Figure 6.1: BESS output for the first month of the Ijpolder case study with the minimum investment model.

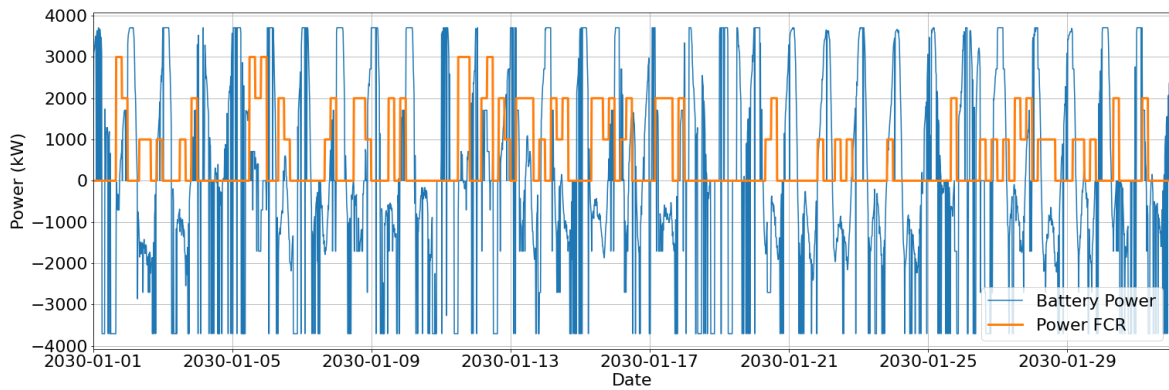


Figure 6.2: BESS output for the first month of the Terschelling case study with the minimum investment model.

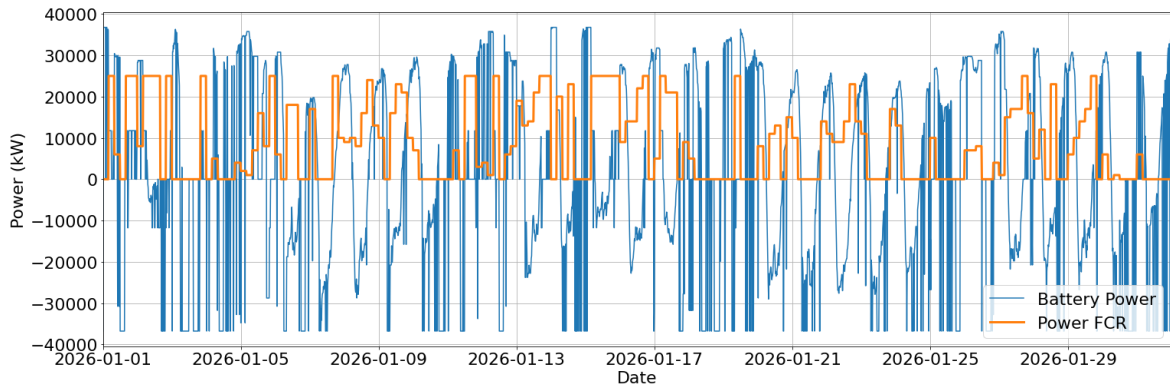


Figure 6.3: BESS output for the first month of the Westhaven case study with the minimum investment model.

Lifetime Evaluation Minimum Investment Model

In this section the lifetime of the different BESSs for the minimum investment model is evaluated. To determine the lifetime of the BESSs, the approach discussed in section 4.3.4 is used. This approach led to the graphs presented in figures 6.4, 6.5 and 6.6.

The end of life of the BESS is assumed to be reached when the total capacity fading line in the graphs passes 80%. In table 6.2 the number of cycles for the different case studies is presented. The graphs show the negative effect of a higher number of cycles. The IJpolder case study has the lowest estimated lifetime with 9.2 years, while the BESS in Terschelling is estimated to reach its end of life after 14.6 years. For the Westhaven case study the battery is estimated to last 30.7 years.

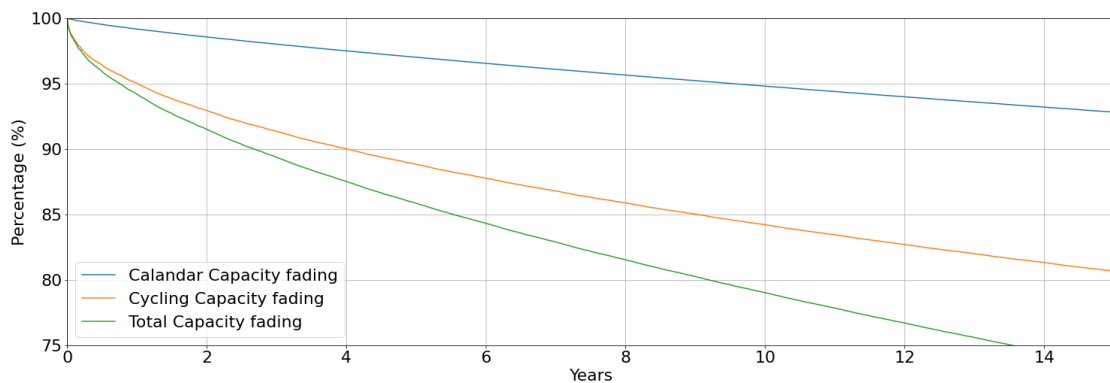


Figure 6.4: Capacity fading of the BESS for the IJpolder case study with the minimum investment model.

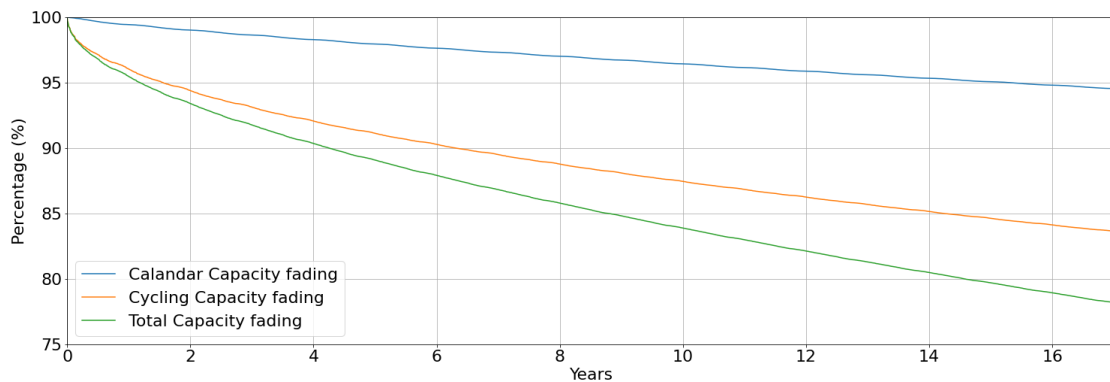


Figure 6.5: Capacity fading of the BESS for the Terschelling case study with the minimum investment model.

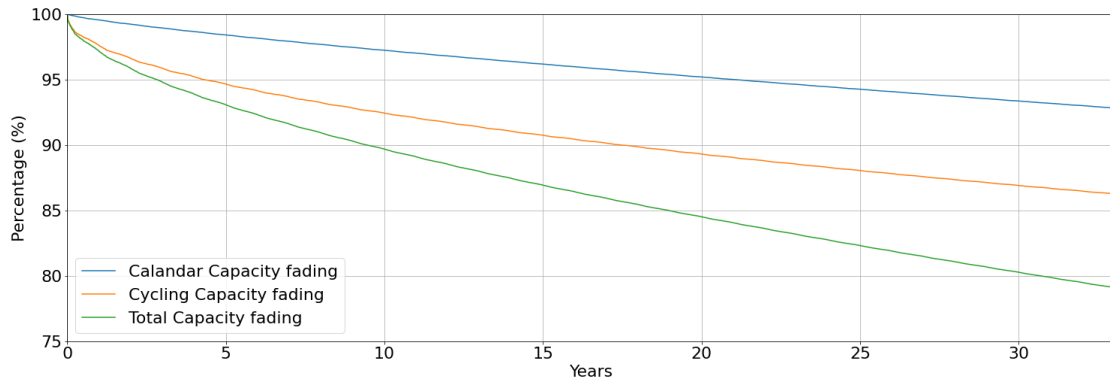


Figure 6.6: Capacity fading of the BESS for the Westhaven case study with the minimum investment model.

6.2 MAXIMUM PROFIT MODEL

The next model that is discussed is the maximum profit model. The goal of this model is to find the size of the BESS such that the profits are maximised. An optimal size is determined, considering the capital costs and the market operations. For this model the parameters from 6.1, the load profiles and the energy prices are used as input. These inputs are used to solve the LP problem presented by 4.10. Because this model arbitrages between the capital costs and the possible market revenue, the amortized costs of capital for one year must be determined. Therefore, an assumption must be made about the lifetime of the BESS. In [56] it is stated that the lifetime of grid connected BESSs peaks between 10 and 11 years for primary frequency regulation. Nevertheless, this number is assumed to be lower in the Netherlands. From the graphs of the capacity fading in section 6.1, it is derived that the minimum end-of-life is reached after 9.2 years. The lifetime of the BESSs in the maximum investment model is assumed to be 8 years, this is a conservative value to limit the risks. The lifetime is used to calculate the amortized costs for power and energy capacity. Dividing the total Capex by the lifetime leads to the following values $18.75 \text{ € per kW-year}$ and $43.75 \text{ € per kWh-year}$. These values are used respectively for the $Capex^P$ and $Capex^E$ in the model. The results of this model are presented in table 6.3. The size of the BESSs are larger than for the minimum investment model. The ratio of the power to energy capacity changes as well, there is a relatively higher power capacity in the maximum profit model.

	IJpolder	Terschelling	Westhaven
Storage Power Capacity (MW)	66.977	28.949	131.325
Storage Energy Capacity (MWh)	44.521	27.573	525.209
Capital costs BESS (Million €)	25.63	13.99	203.52
Profit from imbalance market (Million €)	4.625	1.254	8.160
Profit from FCR market (Million €)	2.529	2.088	2.615
Total profit of market operation (Million €)	7.154	3.334	10.774
Number of Cycles	934	361	181

Table 6.3: The results from the maximum profit model.

Furthermore, the figures 6.7, 5.4 and 6.9 show the BESS output for the different case studies. All BESSs follow the same strategy where the discharging is done in peaks while the charging happens gradually. The output on the FCR market is regularly equal to the maximum indivisible bid.

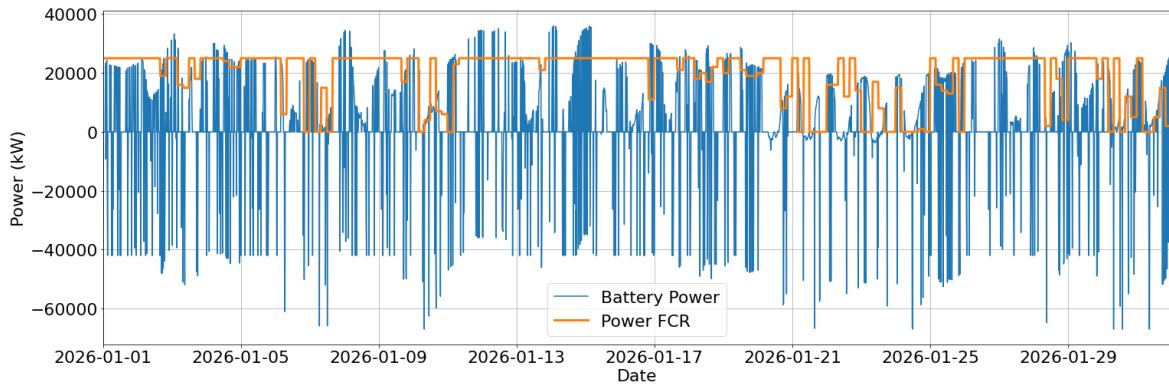


Figure 6.7: BESS output for the first month of the IJpolder case study with the maximum profit model.

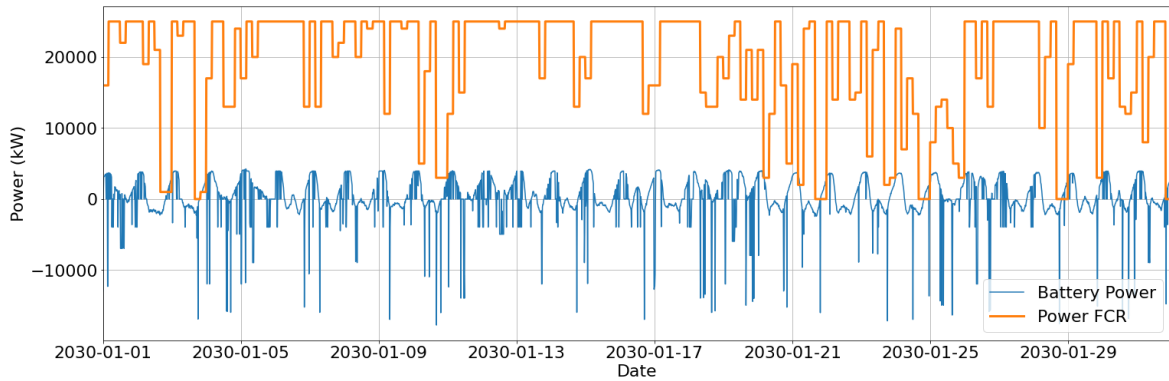


Figure 6.8: BESS output for the first month of the Terschelling case study with the maximum profit model.

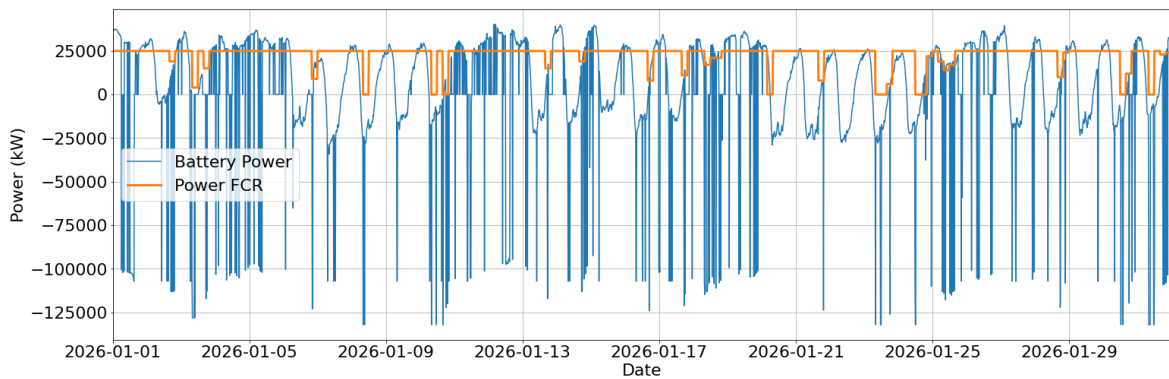


Figure 6.9: BESS output for the first month of the Westhaven case study with the maximum profit model.

Lifetime Evaluation Maximum Profit Model

This section describes the lifetime evaluation of the BESSs in the different case studies using the maximum profit model. The evaluation is executed using the same method as the evaluation for the minimum investment model.

The results of the lifetime evaluation are depicted by figures 6.10, 6.11 and 6.12. The estimated lifetime has decreased for all cases in comparison with the minimum investment model. The IJpolder case study has again the lowest estimated lifetime with a value of 5.2 years, followed by the Terschelling case study with 13.5 years. At last, the lifetime for the Westhaven case study is, similar to the minimum investment model, the highest with 28.8 years. From the graphs is concluded that in terms of battery sizing, the absolute size of the battery does not play a role in the capacity fad-

ing. The ratio between power and energy capacity has the biggest influence on the lifetime estimations.

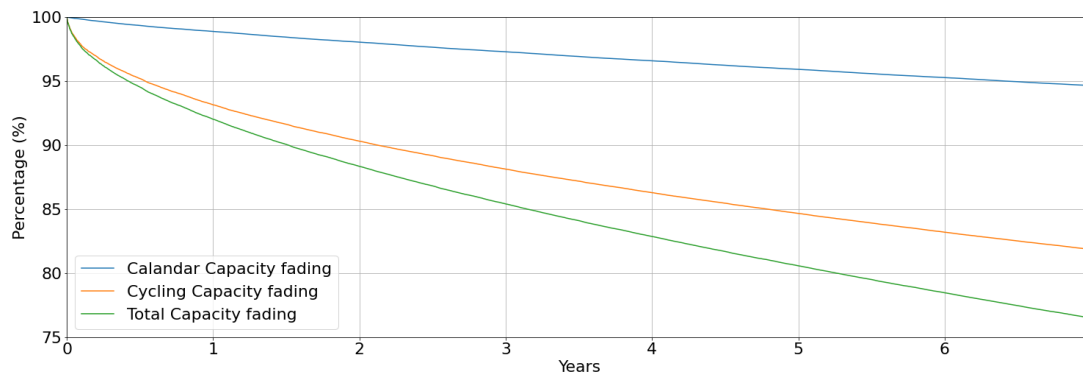


Figure 6.10: Capacity fading of the BESS for the IJpolder case study with the maximum profit model.

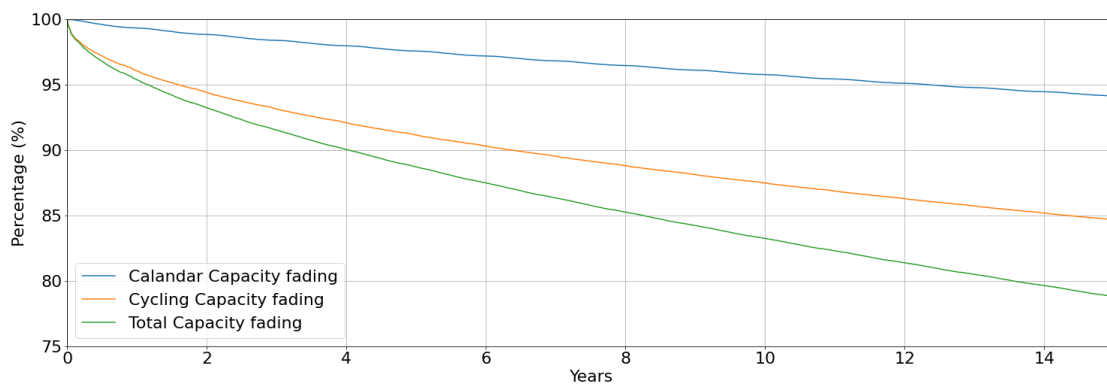


Figure 6.11: Capacity fading of the BESS for the Terschelling case study with the maximum profit model.

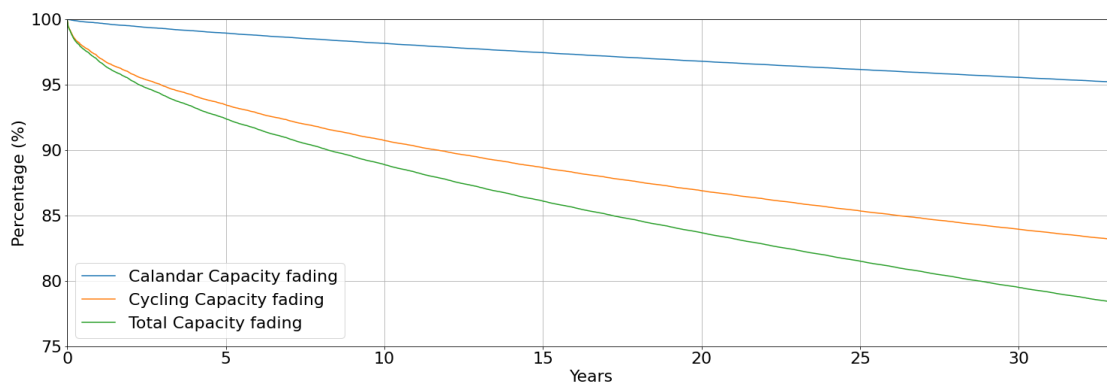


Figure 6.12: Capacity fading of the BESS for the Westhaven case study with the maximum profit model.

6.3 MODEL COMPARISON

To compare the two models, table 6.4 is presented. This table compares outcomes of the different models for the different scenarios. The table compares the capital costs and the total profits from market operations. Furthermore, the cost offset is presented which describes how much of the initial investment is earned back during the first year of operations. At last, the lifetime estimations derived from the capacity fading are compared.

Table 6.4 shows that in all cases the maximum profit model has a lower lifetime estimation than the minimum investment model. This is caused by the higher number of cycles, which is mainly

Scenario	Metric	Minimum Investment Model	Maximum Profit Model
Ijpolder	Total Capital Costs (Million €)	6.22	25.63
	Total profits (Million €)	0.868	7.154
	Cost offset (%)	14	28
	Lifetime estimation (yrs)	9.2	5.2
Terschelling	Total Capital Costs (Million €)	10.21	13.99
	Total profits (Million €)	0.907	3.334
	Cost offset (%)	9	24
	Lifetime estimation (yrs)	14.5	13.6
Westhaven	Total Capital Costs (Million €)	189.34	203.52
	Total profits (Million €)	5.833	10.774
	Cost offset (%)	3	5
	Lifetime estimation (yrs)	30.7	28.8

Table 6.4: Comparison of the minimum investment model and the maximum profit model.

the result of the higher ratio of power capacity to energy capacity. The cost offset is the lowest for the Westhaven model, as this is the case study with the largest amount of congestion. Furthermore, all cases have higher values for the cost offset with the maximum profit model than with the minimum investment. The difference of cost offset is for the Westhaven case study the lowest, as the severity of congestion leaves the least amount of space for an increase in profitability of the BESS between the two models.

6.4 UNCERTAINTY MINIMUM INVESTMENT MODEL

For the uncertainty minimal sizing model the parameters presented in table 6.1 are used together with the load scenarios and the price scenarios. Firstly, the minimal sizes for the BESSs to relieve the congestion with a probability of 99% is determined. To accomplish this, the model proposed by 4.12, is used together with the different load profiles. As stated in section 5.0.2, the standard deviation of the load is assumed to be 200 kW.

After determining the minimum sizes of the BESSs, model 4.14 is used to determine the maximum profit from market operation while considering the probability of occurrence of the different scenarios. The different scenarios for the imbalance prices and FCR prices and the different scenarios are discussed in chapter 5. The results of this model are presented in table 6.5.

	Ijpolder	Terschelling	Westhaven
Storage Power Capacity (MW)	4.191	3.306	37.229
Storage Energy Capacity (MWh)	20.375	75.222	565.769
Capital costs BESS (Million €)	7.760	26.823	203.604
Profit from imbalance market (Million €)	0.798	0.759	4.256
Profit from FCR market (Million €)	0.164	0.069	1.521
Total profit of market operation (Million €)	0.963	0.829	5.777

Table 6.5: The results from the minimum investment model while considering uncertainty.

The difference in sizing between the model that accounts for uncertainty and the model that considers perfect foresight can be determined by comparing the results in table 6.5 and the results in table 6.2. Nevertheless, the difference between the profits from market operation can not be determined using the same results as the sizes of BESSs are different. Therefore, the sizes presented in table 6.5 are used to solve the LP problem 4.10 presented in section 4.2.2. The results of this approach are presented in table 6.6

The results in tables 6.5 and 6.6 show that especially the sizing of the BESSs is influenced by the introduction of uncertainty in the forecast. The Terschelling case study shows the biggest increase

	IJpolder	Terschelling	Westhaven
Storage Power Capacity (MW)	4.191	3.306	37.229
Storage Energy Capacity (MWh)	20.375	75.222	565.769
Capital costs BESS (Million €)	7.760	26.823	203.604
Profit from imbalance market (Million €)	1.073	0.819	5.462
Profit from FCR market (Million €)	0.092	0.065	1.137
Total profit of market operation (Million €)	1.165	0.884	6.599

Table 6.6: The results from the maximum profit model without considering uncertainty.

in size. The uncertainty has big consequences for the minimum size of the BESS to relieve congestion as the uncertainty has the highest relative value for this case study. The comparison of the two tables presents the influence of uncertainty on the profits. In all cases, the total profits are lower when the uncertainty is considered.

6.5 RISK-BASED MAXIMUM PROFIT MODEL

The last model is the risk-based maximum profit model. This model uses the three different load scenarios, the three scenarios for FCR prices and the three scenarios for imbalance prices. All this scenarios are used as the input for the MILP problem presented by 4.16. Like the maximum profit model, this model determines the size based on the capital costs and the potential profit from market participation. Therefore, the amortized costs have to be used again.

Due to the different scenarios and the complexity of the model, problems occurred while trying to run the model for the entire year. The computational burden to run the model was too large. To limit the computational power required, this model is solely run for a part of the year. For the IJpolder and Terschelling case study this came down to the first month of the year, for the Westhaven case study the model was able to run for the first half of the year. This makes it impossible to compare the results of this model with the other models. Nevertheless, the effect of risks on the BESS sizing can be investigated.

The lifetime of the different BESS systems is again assumed to be 8 years, this leads to the amortized costs to be 1.54 € per kW per 30 days for power capacity and 3.60 € per kWh for energy capacity. For the Westhaven model the amortized costs are 21.88 € per kWh and 9.38 € per kW.

Furthermore, the confidence interval β is chosen to be 95%. The value of ω indicates the risk level for the BESS owner, where $\omega = 0$ describes a risk averse profile, while $\omega = 1$ indicates a risk prone profile. The results of this optimisation are given in figures 6.13, 6.14 and 6.15. In these graphs the profit/loss gives the difference between the profit from market operations and the amortized costs of storage. The cost offset represents the amount of amortized storage costs that is offset by the profits from market participation.

The graphs show the same trend for the IJpolder and Terschelling case studies. In both cases the BESS is able to generate profit even when the most risk averse strategy is chosen, leading to a CVaR of zero for all risk levels. This results in a constant battery sizing and profit for all risk levels higher than $\omega=0$. The possibility of a CVaR of zero leads to the model solely optimizing the profits from market operations.

The Westhaven case study shows a completely different trend, as the model is not capable of generating a profitable business case for all risk levels. For this case study the sizing changes for all risk levels and so does the profit and the CVaR. As the model, only runs for half a year and the number of scenarios is limited, the changes are relatively small. To make this changes visible figure 6.16 is introduced. Here the changes of the important values is presented in comparison to the values at $\omega=0$. The graphs show that the introduction of a small amount of risk has the highest influence on the results of the case study. For the higher risk levels, the CVaR and storage costs increase relatively more than the loss decreases.

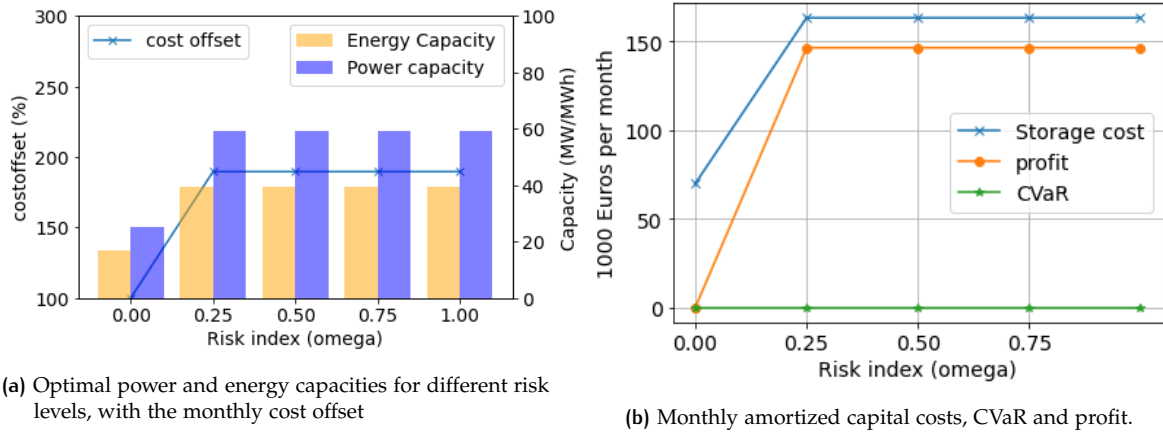


Figure 6.13: Results of the risk-based maximum profit model for the first month of the IJpolder scenario.

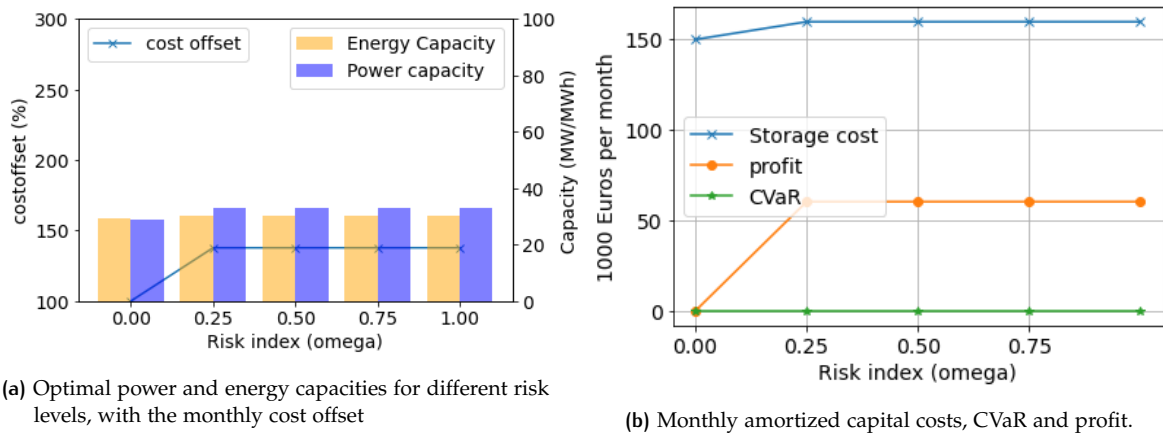


Figure 6.14: Results of the risk-based maximum profit model for the first month of the Terschelling scenario.

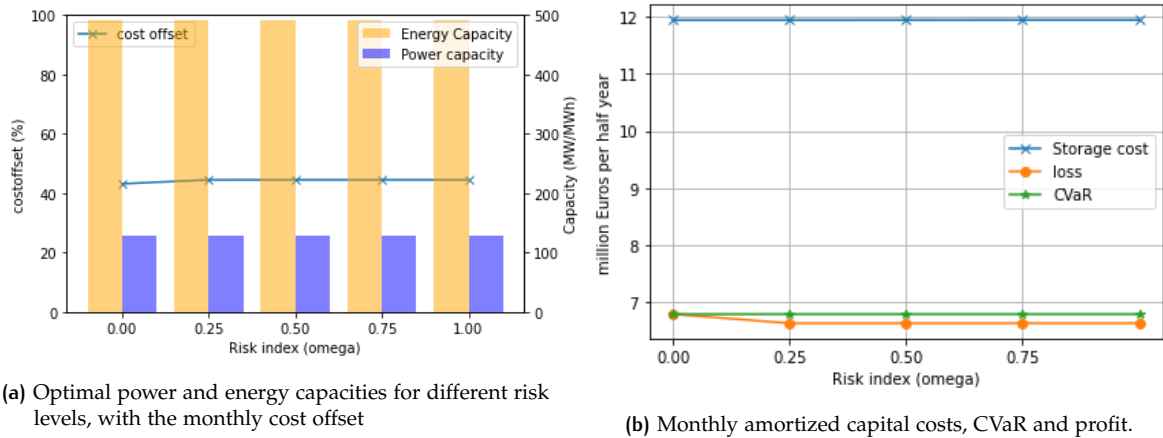
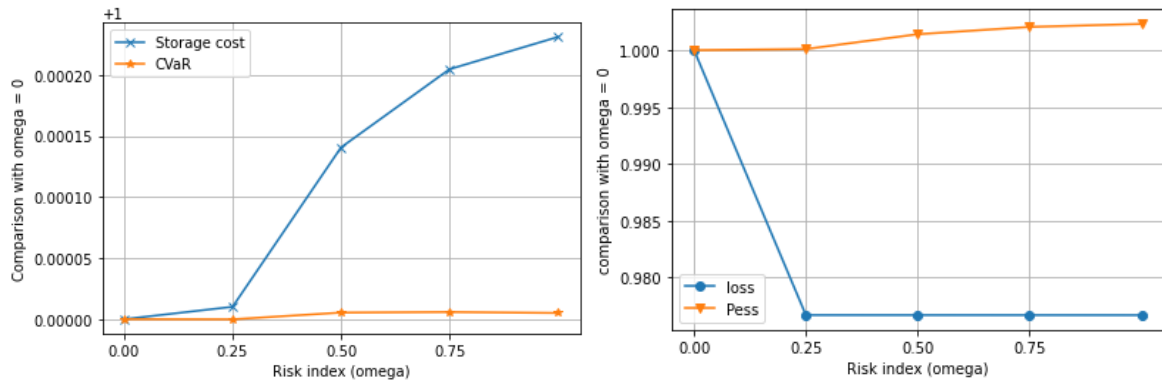


Figure 6.15: Results of the risk-based maximum profit model for the first half year of the Westhaven scenario.



(a) Comparison of the storage costs and CVaR for different risk levels. (b) Comparison of the loss and power capacity for different risk levels.

Figure 6.16: Change in values for different risk levels for the first half year of the Westhaven case study.

7

DISCUSSION

In this chapter a reflection on the results of the different models for the different case studies is given. Firstly, in section 7.1, the results of the minimum investment model are discussed. Secondly, the results of the maximum profit model are analysed in section 7.2. Thereafter, section 7.3 provides an analysis of the uncertainty minimum investment model. At last, in section 7.4 the results of the risk-based maximum profit model are discussed.

7.1 MINIMUM INVESTMENT MODEL ANALYSIS

The results of the minimum investment model are presented in section 6.1. For clarity, table 7.1 summarises the most important parameters used in this model. This table demonstrates that more severe and more frequent congestion leads to higher capital costs of the battery. The predicted congestion at the Westhaven station is the most severe. Therefore, the largest BESS is required to relieve congestion. In theory, a larger BESS could benefit from the larger volumes that could be traded on the markets. It is clear that the BESS in the Westhaven scenario generates the most profit from market operation, as the traded volumes are the biggest. Nevertheless, the total time that congestion occurs, influences the possibilities of the market participation of the BESS. This is demonstrated by the fact that for the Westhaven case study the ratio between BESS size and profit is lower than for the other two cases. The same applies to the comparison between IJpolder and Terschelling.

A payback time is added to the model, for which the profits from market operations are assumed to remain unchanged over the years. This is an unrealistic assumption, because battery degradation, market development and load development are neglected as this is considered outside the scope of this thesis. Nevertheless, it provides a value that can be used to estimate if the BESS could be a profitable business case.

Comparing the payback times to the lifetime estimations provides an insight into the economic feasibility of the business case. A larger lifetime than payback time indicates that the BESS generates profit. For the IJpolder and Terschelling case studies the payback time is lower than the lifetime estimation, indicating a profitable business case. For the Westhaven case study the lifetime estimation is lower than the pay back time, indicating that this business case cannot be profitable without financial remuneration from the DSO for the congestion relief.

It should be considered that this model is based on perfect foresight, which means that the profits indicate unrealistic maximums. Furthermore, especially for the larger BESSs, the price-taker assumption is not realistic, as the large volumes would disrupt the market. Moreover, the lifetime estimations are solely based on the capacity fading due to operations on the imbalance market. Neglecting the operation on the FCR market leads to an overestimation of lifetime of the BESS. Nevertheless, it is assumed that the capacity fading from energy arbitraging on the imbalance market is considerably larger than the capacity fading from the operation on the FCR market. The lifetime estimations are in line with the expected lifetime of the Wärtsilä battery used by Giga Storage, except the Westhaven case study. Giga Storages Buffalo battery should last at least 15 years, if the amount of cycles is kept below an average of 1.8 per day.

In conclusion, the results show that the minimal profit model could in theory provide a profitable business case for the IJpolder and Terschelling case study. Nevertheless, the profitability of the

business case depends on the accuracy of the forecasts and the quality of the trading algorithm. This governs the percentage of the theoretical maximal possible profit from the market could be realised. For the Westhaven case study it is not possible to create a profitable business case without monetary compensation for the relief of congestion. For this case study the payback time is larger than the lifetime estimation of the BESS, hence even with perfect foresight a profitable business case is not possible.

	IJpolder	Terschelling	Westhaven
Total energy that could not be transported (MWh)	103	960	26322
Total time congestion occurs (hrs)	76	1074	2265
Capital Cost of the Bess (Million €)	6.22	10.21	189.34
Profit from market operation (Million €)	0.868	0.907	5.833
Payback time (yrs)	7.17	11.26	32.46
Lifetime estimation (yrs)	9.2	14.5	30.7

Table 7.1: Summary of important number for the minimum investment model

7.2 MAXIMUM PROFIT MODEL ANALYSIS

In section 6.2 the results of the maximum profit model are presented. To summarise the results of the model, table 7.2 is presented. The table includes the financial results and again the payback time. This payback time is again based on the assumption that the profit stays constant each year. Furthermore, the lifetime estimation is presented in the table.

To analyse the results of this model, a comparison should be made with the minimum investment model. From this comparison it is evident that the minimal BESS size is not the most profitable, as for all case studies the size of the BESSs increases for the maximum profit model. Another interesting observation can be made in the ratio between power and energy capacity. All case studies have relatively more power capacity than in the minimum investment model, which increases the possibility to trade large volumes of energy for a short period of time. For the Terschelling and Westhaven case studies, the size of the energy capacity is the same in both scenarios, as the energy capacity required to relieve congestion has already surpassed the point at which profit increases with capacity. The payback time for all case studies has decreased, as the increase in profits from market operations outweighs the increase in capital costs. Furthermore, the lifetime estimation of all models has decreased because the change in ratio between power and energy capacity results in a more severe cycling pattern.

This model has the same unrealistic characteristics as the minimum investment model, as it is based on perfect foresight. Moreover, with the increasing size of the BESS, the assumption that there is enough space near the substation and enough capacity on the substation becomes more unrealistic, especially since IJpolder and Westhaven are located near the centre of Amsterdam and Terschelling is merely a small island. In addition, to determine the amortized costs of storage a lifetime of 8 years is assumed. However, the lifetime estimations all differ from this number. This leads to a size optimisation based on unrealistic capital costs. Nevertheless, an assumption has to be made and 8 years is assumed to be reasonably conservative.

For the maximum profit model the lifetime estimation is higher than the payback time for all cases, indicating the feasibility of a profitable business case. Nevertheless, this depends on the accuracy of the forecasts and the quality of the trading strategy in the same way as for the minimum investment model. Especially the Terschelling case study seems promising with a payback time of 4.2 years and a lifetime estimation of 13.6. For the Westhaven case study it should be considered that a lifetime of 28.8 years is highly unlikely. If a more realistic lifetime estimation is assumed this business case would not be profitable. Therefore, the lifetime of this case study should be investigated more in-depth.

	Ijpolder	Terschelling	Westhaven
Capital Cost of the Bess (Million €)	25.63	13.99	203.52
Profit from market operation (Million €)	7.154	3.334	10.774
Payback time (yrs)	3.58	4.20	18.89
Lifetime estimation (yrs)	5.2	13.6	28.8

Table 7.2: Summary of the financial results of the maximum investment model.

7.3 UNCERTAINTY MINIMUM INVESTMENT MODEL ANALYSIS

The results of the uncertainty minimum investment model are presented in section 6.4. Again, to make a good analysis of the results of this model, the results should be compared to that of the minimal sizing model.

Evident from the comparison is that the sizing of the BESS is strongly influenced by the introduction of uncertainty, especially for the Terschelling case study. As the capacity and load are relatively low, the small uncertainty has relatively large consequences for the sizing. The standard deviation is assumed the same for all case studies, while in reality this would not be the case. Therefore, the uncertainty has the largest influence on the case study with the lowest capacity, namely Terschelling. Because no data is available to determine the standard deviation, this is assumed to be the same for all case studies. A call with Liander led to the conclusion that even the DSO is uncertain about the accuracy of their forecasts, as these are based on many variables.

The profit generated by the BESSs for the different case studies is lower for all cases when uncertainty is considered. As a consequence of the way in which the different case studies are defined. The profit is determined by the average of the scenarios considering their probability of occurrence. By assuming that the load forecast follows a normal distribution, the probability of a higher or lower value than the predicted value is the same. The different price scenarios are assumed to have the same probability of occurrence. Figure 5.7 and 5.8 give the average prices for the two years that are studied. The average prices show that the high and mid price are more similar than the mid and low price, especially in FCR. With the assumption that all the price scenarios have the same probability of occurrence, this leads to lower profits from market operations. Nevertheless, this model provides an insight into the influence of uncertainty in forecasts and the influence of the way different scenarios are defined. To improve this model it would be beneficial to study the probability density functions of the forecasts in more detail and to consider more scenarios. However, this is considered outside the scope of the thesis.

7.4 RISK-BASED MAXIMUM PROFIT ANALYSIS MODEL

The last results that are analysed are those resulting from the risk-based maximum profit model. The results are presented by the graphs in section 6.5. Unfortunately, the complexity and the many integer variables created a too large computational burden to run the model for the whole year on the computer at hand. Therefore, it was decided to run the model for only a part of the the year; i.e. the first month of the Terschelling and Ijpolder case study and the first half year of the Westhaven case study. The difference in simulated time makes it impossible to compare the results of this model to the results of the other models.

Nevertheless, the effect of risk on the model can be analysed. For the Ijpolder and Terschelling case studies was found that the size of BESS does not change if the risk factor exceeds 0.25. However, the sizes change as the risk factor is increased from zero. The model is able to generate profit with the most risk averse profile, resulting in a CVaR of zero for all risk levels. The CVaR of zero causes the model to solely optimise for the BESS size, when the risk level is higher than zero.

For the Westhaven case study the results are different; in this case study the model is not able to achieve a profitable BESS for any of the assessed risk levels. This leads to a different profile and

for change of all values, when the risk level is increased. The energy capacity remains constant as increasing this does not translate to a decrease in losses. Due to the limited number of scenarios and the limited time scope of the model the differences of the results, for the different risk factors, are small. Nevertheless, figure 6.16 shows that the introduction of risk has more impact on the profitability than increasing this risk. The difference between the results of no risk and a small risk are larger than the difference of result for the higher risk levels.

This model is again dependent on the chosen amortized costs of the BESS, in which, again, a lifetime of eight years was assumed. To generate a more precise prediction for a case study a more in-depth analysis of the amortized cost is required. Nevertheless, this was considered outside the scope of this thesis, as this is dependent on a complex set of unknown variables. At last, this model is able to provide a better understanding on the influence of monetary risks on the optimisation of the BESS.

8

CONCLUSION

In this chapter the conclusion of the report is presented. The research questions are stated, followed by the answers. The answers are based on the findings presented in the report. Firstly, the sub-questions are discussed. Thereafter, the main research question is answered.

Is it possible to develop a model that optimises the size of a BESS to relieve congestion, while generating revenues on the electricity market?

In chapter 3 is discussed that extensive research is done into this subject and that the possibility is there. This is proven by the models presented in chapter 4. Four different models are developed that optimise the sizing of a BESS that participates in the FCR and imbalance market, while relieving congestion. All four models were successfully in relieving the congestion and generating profit on the markets. The models differ in their modeling philosophy. The minimum investment models determine the minimal size to relieve congestion, while the maximum profit model determines the optimal size to generate the highest amount of profit. The uncertainty model incorporates the uncertainty of forecasts, the same goes for the risk-based maximum profit model, which additionally adds a risk factor. In conclusion, the answer to this question is yes.

What is the influence of the severity of the congestion on the profitability of a congestion relieving BESS?

To answer this question, the results of the minimum investment model and the maximum profit model must be analysed. These results are presented in sections 6.1 and 6.2. To understand the influence of the severity of congestion on the profitability of the BESS, the different case studies are compared. At the Westhaven station the congestion is most severe, which leads to the biggest size BESS. Nevertheless, the severity of the congestion causes that during long periods the BESS cannot fully participate in the market. Therefore, as discussed in chapter 7, the payback period of this BESS is the longest of the three case studies. For this case study it is not possible to generate enough profit on the imbalance and FCR market to achieve a financially viable business case without remuneration for the congestion relief from the DSO. The IJpolder case study endures the least severe congestion and for this case study the payback period for the two models is the shortest. The severity of congestion for the Terschelling case study is between the other two and so does the payback period of the BESS. Nevertheless, if the lifetime estimation is considered the Terschelling case study has the highest profitability. From these results it could be concluded that the severity of congestion has a considerable negative influence on the profitability of the BESS, especially if the degradation is not considered. In extreme severe cases like Westhaven, the severity of congestion makes it even impossible to achieve a profitable business case for a BESS, without monetary compensation for the relieved congestion. In less severe cases the amount of congestion has less influence on the profitability of the BESS.

What is the influence of uncertainty in market and load forecasts on the sizing and revenue of a BESS?

The answer to this question can be found by comparing the results of the minimal sizing model and the uncertainty minimal sizing model. These results are presented in sections 6.1 and 6.4. From these results it becomes clear that introducing uncertainty leads to bigger BESS sizing. Looking at the different case studies, it can be concluded that a relatively higher uncertainty leads to more

severe influences on the sizing. As the uncertainty for all case studies is assumed to be the same, the relative uncertainty for the Terschelling case study is the highest. This results in the biggest increase in size of the BESS.

The influence of the different scenarios in profit generated from the market is found in tables ?? and 6.6. The introduction of the uncertainty leads to a lower total profit from market operations. This gives a more realistic prediction of the profit that the BESS can generate, as in reality the trading strategy is also based on uncertain forecasts. Comparing the IJpolder and Westhaven case study, which use the same electricity prices, shows that influence on the smaller BESS is relatively bigger than on the bigger BESS of the Westhaven case study. Nevertheless, the absolute change in total profit is bigger for the the Westhaven case study.

In conclusion, the introduction of uncertainty leads in all cases to higher investment costs for the BESS to relieve congestion and to lower profits from market operations. Furthermore, higher relative uncertainty of the forecasts lead to more severe consequence. Thus, the uncertainty has a negative influence in the profitability of the business case and more accurate forecasts lead to a stronger business case.

What is the influence of monetary risks taken by the BESS owner on the sizing and revenue of a BESS?

To asses this question the risk-based maximum profit model is developed. Unfortunately, due to lack of computational power it was not possible to run simulation for a whole year. Nevertheless, based on the results of the model this question can be answered. In all cases, it appeared to be more profitable to take some risk than to choose the complete risk averse strategy. Though, for the Terschelling and IJpolder case study the value for for the CVaR was zero in all cases. Therefore, the financial risks of a more risk prone strategy could not be determined.

However, the results of the Westhaven case study show the introduction of risk has a more beneficial result on the profitability of the business case than increasing that risk. As for the higher risk levels the decrease in loss was lower than for the step from $\omega = 0$ to $\omega = 0.25$, while the increase in CVaR was bigger and capital costs were bigger.

This leads to the conclusion that taking risks is beneficial for the business case, whereby the most benefit is obtained by the increase between the lower risk levels.

Is it possible to create a profitable business case for grid connected BESS that relieves local congestion on the Dutch electricity grid, while generating profit through market operations?

To answer the main research question, the results of all models are analysed. The results show that for the IJpolder and Terschelling case study both with the minimum investment model and the maximum profit model a profitable business case would be theoretically possible. For the Westhaven case study, this is not possible with the minimum investment model. With the maximum profit model it seems possible, Though, the lifetime estimation of 29 years seems highly unlikely. Therefore, this case study would benefit from looking into alternatives to relieve the congestion. Nevertheless, for all cases it has to be said that the profitability of the business case is dependent on the quality of the trading strategy and the forecasts. This thesis shows that it is theoretically possible for at least, two of the three case studies to relieve congestion while generation enough profit through market operations.

Therefore, the short answer to the main research question is 'yes'. It is clear that it is possible to create a profitable business case with a BESS that relieves congestion, even if no remuneration is obtained. However, if the congestion is too severe, a financial compensation paid by the DSO to the BESS owner is required to achieve a financially viable business case.

9

RECOMMENDATIONS

In this section recommendations and the future outlook for further research on this subject are provided. These recommendations and future outlook are based on the experience gained by completing this thesis.

Firstly, it would be beneficial to incorporate battery degradation in the model, unlike the current model where the capacity fading is determined based on the results of the model. By incorporating the degradation in the model, the battery sizing can be optimised, while considering degradation. This is beneficial to determine a more realistic prediction of the generated profits as degradation influences the operations. Moreover, the sizing can be determined to, even with degradation, relieve the congestion during the entire lifetime of the BESS. In the current model only the capacity fading of the battery is considered to determine the lifetime of the BESS, while power fading and loss of efficiency are neglected. In future works the incorporation of these aging mechanisms would be beneficial for the accuracy of the results. Furthermore, the influence of the operations on the FCR market are neglected. In future works, this influence should be studied and introduced to the model. Incorporating all the aging effects of the BESS to the model results in a more accurate optimisation of the BESS sizing and a more realistic prediction of the BESS profit generating capabilities.

It is discussed that there are many different possible revenue streams for a grid connected BESS. Nevertheless, in this thesis solely the stacking of the FCR and imbalance market is discussed. In future research, the stacking of all different revenue streams should be investigated. The future works should investigate if it is possible to achieve a more profitable business case through the stacking of different revenue streams. Currently, especially the aFFR market seems to be an interesting opportunity.

While investigating other possible revenue streams, monetary compensation for relieving congestion should be considered. In this thesis no remuneration for the congestion relief of the BESS is determined. In real reality, the BESS owner would demand a compensation for this service. The Dutch DSO's have introduced GOPACS to create a market for congestion relief. Nevertheless, the service as described in this thesis would be agreed upon with the DSO outside of GOPACS. To estimate the monetary worth of this service, future works should assess the costs of congestion. This could lead to a better understanding of the value of this service, which would be beneficial for the BESS owner and the DSO. Determining a fair price for the relief of structural congestion is required to further develop this solution.

The models in this thesis use input data with a maximum interval of one year. Therefore, the results are based on the scope of one year. If the battery degradation is included in the models it would be beneficial to run the models over the whole lifetime of the BESS. The BESS owner would get a more detailed insight of the influence of degradation of the BESS over its lifetime and a more accurate lifetime estimation of the BESS as the cycle patterns differ over the years. To accomplish this more computational power would be required and the load and price data for the entire lifetime of the BESS should be available.

This thesis presents two models based on the assumption of perfect foresight of the future load profiles and energy prices. These models present the theoretical maximum profit that could be achieved through market operations. To gain knowledge on the percentage of this profit that could

be realised, research should be done into different trading strategies and algorithms. Understanding of the performance of the different trading algorithms and strategies is essential to determine the accuracy of the profits predicted by these models.

At last, two models where uncertainty is considered are presented in this Thesis. To increase the accuracy of these models, research should be done into the accuracy of load and price forecasts. The future research should aim to construct accurate probability density functions for these forecasts. Part of this research should be on the influence of the time horizon on the accuracy of the forecasts as long-term forecasts are generally less accurate than short-term forecasts. Incorporating these modified uncertainties in the model would lead to more accurate results. Furthermore, if more computational power is available, a larger sample size of different price and load scenarios should be investigated to increase the accuracy.

BIBLIOGRAPHY

- [1] Netbeheer nederland capacity charts. <https://capaciteitskaart.netbeheernederland.nl/>. "Accessed: 2022-06-21".
- [2] Marco Stecca, Laura Ramirez Elizondo, Thiago Batista Soeiro, Pavol Bauer, and Peter Palensky. A comprehensive review of the integration of battery energy storage systems into distribution networks. *IEEE Open Journal of the Industrial Electronics Society*, 1:46–65, 2020.
- [3] Mostafa H. Mostafa, Shady H.E. Abdel Aleem, Samia G. Ali, Ziad M. Ali, and Almoataz Y. Abdelaziz. Techno-economic assessment of energy storage systems using annualized life cycle cost of storage (lccos) and levelized cost of energy (lcoe) metrics. *Journal of Energy Storage*, 29:101345, 6 2020.
- [4] Luca Argiolas. Optimization of battery energy storage system operation in distribution grids. 07 2021.
- [5] Netbeheer Nederland. Basisinformatie over energie-infrastructuur. 2019.
- [6] <https://www.tennet.eu/nl/balanceringsmarkten>. Accessed: 2022-08-26.
- [7] <https://www.thinkingondata.com/normal-distribution-what-means-in-numbers/>. Accessed: 2022-08-28.
- [8] Meisam Farrokhifar, Farid Hamzeh Aghdam, Arman Alahyari, Ali Monavari, and Amin Safari. Optimal energy management and sizing of renewable energy and battery systems in residential sectors via a stochastic milp model. *Electric Power Systems Research*, 187:106483, 10 2020.
- [9] Congestiegebied ijpolder. <https://www.liander.nl/sites/default/files/20220512%20Vooraankondiging%20verdeelstation%20Ijpolder%20v.1.1.pdf>. Accessed: 2022-08-28.
- [10] Vooraankondiging verwachte congestie verdeelstation herbayum. <https://www.liander.nl/sites/default/files/20200123%20Vooraankondiging%20verwachte%20congestie%20verdeelstation%20Herbayum%20V1.0.pdf>. Accessed: 2022-08-28.
- [11] Congestiegebied westhaven. <https://www.liander.nl/sites/default/files/20210930%20Vooraankondiging%20O5%20Westhaven%20v1.2.pdf>. Accessed: 2022-08-28.
- [12] Watts up: Dutch electric grid is at capacity. <https://www.dutchnews.nl/news/2021/09/watts-up-dutch-electric-grid-is-at-capacity/>. Accessed: 2022-09-01.
- [13] Hans Schermeyer, Michael Studer, Manuel Ruppert, and Wolf Fichtner. Understanding distribution grid congestion caused by electricity generation from renewables. pages 78–89, 09 2017.
- [14] Silvia Martinez Romero and Wendy Hughes. Bringing variable renewable energy up to scale options for grid integration using natural gas and energy storage. 2015.
- [15] Alexander W. Dowling, Ranjeet Kumar, and Victor M. Zavala. A multi-scale optimization framework for electricity market participation. *Applied Energy*, 190:147–164, 2017.
- [16] Juan Arteaga, Hamidreza Zareipour, and Nima Amjady. Energy storage as a service: Optimal sizing for transmission congestion relief. *Applied Energy*, 298, 9 2021.
- [17] Janine Paulusse (ECONNETIC) Eelco Rondhuis (ECONNETIC), Karen Friele (ECONNETIC) and Hage de Vries (ECONNETIC). De financierbaarheid van een batterij in een gesloten distributie systeem. 3 2021.

- [18] Matthias Pauw. Overschot groene stroom kost tennet honderden miljoenen, burgers betalen. <https://www.rtlnieuws.nl/economie/artikel/5312211/tennet-stroomnet-hoogspanning-congestie-kosten-honderden-miljoenen>, 2022. Accessed: 2022-06-21.
- [19] Martti J. van Blijswijk and Laurens J. de Vries. Evaluating congestion management in the dutch electricity transmission grid. *Energy Policy*, 51:916–926, 2012. Renewable Energy in China.
- [20] Raymond H. Byrne, Tu A. Nguyen, David A. Copp, Babu R. Chalamala, and Imre Gyuk. Energy management and optimization methods for grid energy storage systems. *IEEE Access*, 6:13231–13260, 2018.
- [21] Fatemeh Rostami, Zoltán Kis, Rembrandt Koppelaar, Laureano Jiménez, and Carlos Pozo. Comparative sustainability study of energy storage technologies using data envelopment analysis. *Energy Storage Materials*, 48:412–438, 6 2022.
- [22] Abraham Alem Kebede, Theodoros Kalogiannis, Joeri Van Mierlo, and Maitane Berecibar. A comprehensive review of stationary energy storage devices for large scale renewable energy sources grid integration. *Renewable and Sustainable Energy Reviews*, 159, 5 2022.
- [23] Surender Reddy Salkuti. Energy storage technologies for smart grid: A comprehensive review. *Majlesi Journal of Electrical Engineering*, 14:39–48, 3 2020.
- [24] Kamil Khuwaja. 2013 electricity storage handbook in collaboration with nreca.
- [25] Xing Luo, Jihong Wang, Mark Dooner, and Jonathan Clarke. Overview of current development in electrical energy storage technologies and the application potential in power system operation. *Applied Energy*, 137:511–536, 1 2015.
- [26] Kyle Bradbury. Energy storage technology review. 2010.
- [27] P. Kurzweil. History | secondary batteries. *Encyclopedia of Electrochemical Power Sources*, pages 565–578, 1 2009.
- [28] Mathew Aneke and Meihong Wang. Energy storage technologies and real life applications – a state of the art review. *Applied Energy*, 179:350–377, 10 2016.
- [29] Julien Matheys, Jean Marc Timmermans, Wout van Autenboer, Joeri van Mierlo, Gaston Maggetto, Sandrine Meyer, Arnaud de Groof, Walter Hecq, and Peter van den Bossche. Comparison of the environmental impact of 5 electric vehicle battery technologies using lca. *Proceedings of the 13th CIRP International Conference on Life Cycle Engineering, LCE 2006*, pages 97–102, 2006.
- [30] Ahmad Arabkoohsar. Classification of energy storage systems. *Mechanical Energy Storage Technologies*, pages 1–12, 2021.
- [31] Siraj Sabihuddin, Aristides E. Kiprakis, and Markus Mueller. A numerical and graphical review of energy storage technologies. *Energies 2015, Vol. 8, Pages 172-216*, 8:172–216, 12 2014.
- [32] Haisheng Chen, Thang Ngoc Cong, Wei Yang, Chunqing Tan, Yongliang Li, and Yulong Ding. Progress in electrical energy storage system: A critical review. *Progress in Natural Science*, 19:291–312, 3 2009.
- [33] Wesley J Cole and Allister Frazier. Cost projections for utility-scale battery storage. 6 2019.
- [34] Marc Beaudin, Hamidreza Zareipour, Anthony Schellenberg, and William Rosehart. Energy storage for mitigating the variability of renewable electricity sources. *Energy Storage for Smart Grids: Planning and Operation for Renewable and Variable Energy Resources (VERs)*, pages 1–33, 2015.

- [35] Amit Kumar Rohit and Saroj Rangnekar. An overview of energy storage and its importance in indian renewable energy sector: Part ii – energy storage applications, benefits and market potential. *Journal of Energy Storage*, 13:447–456, 10 2017.
- [36] Anil Kumar Singh Maisanam, Agnimitra Biswas, and Kaushal Kumar Sharma. An innovative framework for electrical energy storage system selection for remote area electrification with renewable energy system: Case of a remote village in india. *Journal of Renewable and Sustainable Energy*, 12:024101, 3 2020.
- [37] Stephen Mccluer and Jean-Francois Christin. Comparing data center batteries, flywheels, and ultracapacitors revision 2.
- [38] Marc Beaudin, Hamidreza Zareipour, Anthony Schellenberglobe, and William Rosehart. Energy storage for mitigating the variability of renewable electricity sources: An updated review. *Energy for Sustainable Development*, 14:302–314, 12 2010.
- [39] Piergiorgio Alotto, Massimo Guarnieri, and Federico Moro. Redox flow batteries for the storage of renewable energy: A review. *Renewable and Sustainable Energy Reviews*, 29:325–335, 1 2014.
- [40] Choton K. Das, Octavian Bass, Ganesh Kothapalli, Thair S. Mahmoud, and Daryoush Habibi. Overview of energy storage systems in distribution networks: Placement, sizing, operation, and power quality. *Renewable and Sustainable Energy Reviews*, 91:1205–1230, 8 2018.
- [41] Francisco Díaz-González, Andreas Sumper, Oriol Gomis-Bellmunt, and Roberto Villafáfila-Robles. A review of energy storage technologies for wind power applications. *Renewable and Sustainable Energy Reviews*, 16:2154–2171, 5 2012.
- [42] Omid Palizban and Kimmo Kauhaniemi. Energy storage systems in modern grids—matrix of technologies and applications. *Journal of Energy Storage*, 6:248–259, 5 2016.
- [43] Furquan Nadeem, S. M.Suhail Hussain, Prashant Kumar Tiwari, Arup Kumar Goswami, and Taha Selim Ustun. Comparative review of energy storage systems, their roles, and impacts on future power systems. *IEEE Access*, 7:4555–4585, 2019.
- [44] Overview of energy storage methods. 2007.
- [45] C. Ponce de León, A. Frías-Ferrer, J. González-García, D. A. Szánto, and F. C. Walsh. Redox flow cells for energy conversion. *Journal of Power Sources*, 160:716–732, 9 2006.
- [46] Marvin Killer, Mana Farrokhseresht, and Nikolaos G. Paterakis. Implementation of large-scale li-ion battery energy storage systems within the emea region. *Applied Energy*, 260, 2 2020.
- [47] N. Lebedeva, D. Tarvydas, I. Tsiropoulos, and European Commission. Joint Research Centre. Li-ion batteries for mobility and stationary storage applications : scenarios for costs and market growth. 2018.
- [48] Matthew T. Lawder, Bharatkumar Suthar, Paul W.C. Northrop, Sumitava De, C. Michael Hoff, Olivia Leitermann, Mariesa L. Crow, Shriram Santhanagopalan, and Venkat R. Subramanian. Battery energy storage system (bess) and battery management system (bms) for grid-scale applications. *Proceedings of the IEEE*, 102:1014–1030, 2014.
- [49] Behnam Zakeri and Sanna Syri. Electrical energy storage systems: A comparative life cycle cost analysis. *Renewable and Sustainable Energy Reviews*, 42:569–596, 2 2015.
- [50] IEEE. Ieee std 519™-2014: Ieee recommended practice and requirements for harmonic control. *ANSI/IEEE Std. 519*, 2014:5–9, 2014.
- [51] IEEE. Ieee std 1547-2018. *IEEE Standard for Interconnection and Interoperability of Distributed Energy Resources with Associated Electric Power Systems Interfaces*, pages 1–138, 2018.

- [52] Cheng Lin, Aihua Tang, Hao Mu, Wenwei Wang, and Chun Wang. Aging mechanisms of electrode materials in lithium-ion batteries for electric vehicles. *Journal of Chemistry*, 2015, 2015.
- [53] Jorn M. Reniers, Grietus Mulder, and David A. Howey. Review and performance comparison of mechanical-chemical degradation models for lithium-ion batteries. *Journal of The Electrochemical Society*, 166:A3189–A3200, 9 2019.
- [54] Jacqueline S. Edge, Simon O’Kane, Ryan Prosser, Niall D. Kirkaldy, Anisha N. Patel, Alastair Hales, Abir Ghosh, Weilong Ai, Jingyi Chen, Jiang Yang, Shen Li, Mei Chin Pang, Laura Bravo Diaz, Anna Tomaszewska, M. Waseem Marzook, Karthik N. Radhakrishnan, Huizhi Wang, Yatish Patel, Billy Wu, and Gregory J. Offer. Lithium ion battery degradation: what you need to know. *Physical Chemistry Chemical Physics*, 23:8200–8221, 4 2021.
- [55] Thomas Waldmann, Marcel Wilka, Michael Kasper, Meike Fleischhammer, and Margret Wohlfahrt-Mehrens. Temperature dependent ageing mechanisms in lithium-ion batteries - a post-mortem study. *Journal of Power Sources*, 262:129–135, 9 2014.
- [56] Marco Stecca, Thiago Batista Soeiro, Laura Ramirez Elizondo, Pavol Bauer, and Peter Palensky. Lifetime estimation of grid-connected battery storage and power electronics inverter providing primary frequency regulation. *IEEE Open Journal of the Industrial Electronics Society*, 2:240–251, 2021.
- [57] Daniel-Ioan Stroe. Lifetime models for lithium ion batteries used in virtual power plants. 2014.
- [58] Arpit Maheshwari, Nikolaos G. Paterakis, Massimo Santarelli, and Madeleine Gibescu. Optimizing the operation of energy storage using a non-linear lithium-ion battery degradation model. *Applied Energy*, 261:114360, 3 2020.
- [59] https://tennet-drupal.s3.eu-central-1.amazonaws.com/default/2022-09/NL_JUN2022_Onshore_Corporate.pdf. Accessed: 2022-08-02.
- [60] <https://www.energievergelijk.nl/onderwerpen/netbeheerders>. Accessed: 2022-08-02.
- [61] Anne Looijestijn-Clearie. Breaking up is hard to do: Dutch unbundling legislation and the free movement of capital. *European Business Organization Law Review*, 15:337–355, 1 2014.
- [62] Fehmi Tanrisever, Kursad Derinkuyu, and Geert Jongen. Organization and functioning of liberalized electricity markets: An overview of the dutch market. *Renewable and Sustainable Energy Reviews*, 51:1363–1374, 8 2015.
- [63] Eric E.C. van Damme. Liberalizing the dutch electricity market: 1998-2004. *SSRN Electronic Journal*, 12 2011.
- [64] <https://www.tennet.eu/nl/soorten-elektriciteitsmarkten>. Accessed: 2022-08-25.
- [65] Amprion / Apg, Elia / Rte, / Swissgrid, and / Tennet. About epex spot 49% 51% hgrt.
- [66] Battery energy storage systems in the netherlands market opportunities financing challenges, 2021.
- [67] Fcr manual for bsp’s requirements and procedures for supply of fcr. 2022.
- [68] Manual afrr for bsps rules and procedures for afrr delivery. 2022.
- [69] Lazard. Lazard’s leveled cost of storage analysis - version 5.0. 11 2019.
- [70] Ying Jun Angela Zhang, Changhong Zhao, Wanrong Tang, and Steven H. Low. Profit-maximizing planning and control of battery energy storage systems for primary frequency control. *IEEE Transactions on Smart Grid*, 9:712–723, 2018.
- [71] Koen Broess Winifred Roggekamp Wilbert Prinssen Novy Francis, Rianne ’t Hoen. Smart grid ready energy storage. 2 2020.

- [72] Luca Argiolas, Marco Stecca, Laura M. Ramirez-Elizondo, Thiago Batista Soeiro, and Pavol Bauer. Optimal battery energy storage dispatch in energy and frequency regulation markets while peak shaving an ev fast charging station. *IEEE Open Access Journal of Power and Energy*, 9:374–385, 2022.
- [73] Yuqing Yang, Stephen Bremner, Chris Menictas, and Merlinde Kay. Battery energy storage system size determination in renewable energy systems: A review. *Renewable and Sustainable Energy Reviews*, 91:109–125, 8 2018.
- [74] Jason Leadbetter and Lukas G. Swan. Selection of battery technology to support grid-integrated renewable electricity. *Journal of Power Sources*, 216:376–386, 10 2012.
- [75] Xiayue Fan, · Bin Liu, Jie Liu, Jia Ding, · Xiaopeng Han, Yida Deng, · Xiaojun Lv, Ying Xie, Bing Chen, Wenbin Hu, and · Cheng Zhong. Battery technologies for grid-level large-scale electrical energy storage. 26:92–103, 1234.
- [76] Tianmei Chen, Yi Jin, Hanyu Lv, Antao Yang, Meiyi Liu, Bing Chen, Ying Xie, and Qiang Chen. Applications of lithium-ion batteries in grid-scale energy storage systems, 6 2020.
- [77] S. A.R. Mir Mohammadi Kooshknow and C. B. Davis. Business models design space for electricity storage systems: Case study of the netherlands. *Journal of Energy Storage*, 20:590–604, 12 2018.
- [78] Raymond H. Byrne, Tu A. Nguyen, David A. Copp, Babu R. Chalamala, and Imre Gyuk. Energy management and optimization methods for grid energy storage systems. *IEEE Access*, 6:13231–13260, 8 2017.
- [79] L Fiorini, G ; Pagani, P ; Pelacchi, D ; Poli, and M ; Aiello. Sizing and siting of large-scale batteries in transmission grids to optimize the use of renewables. *IEEE Journal on Emerging and Selected Topics in Circuits and Systems*, 7:285–294, 2017.
- [80] Clémentine Straub, Jean Maeght, Camille Pache, Patrick Panciatici, and Ram Rajagopal. Congestion management within a multi-service scheduling coordination scheme for large battery storage systems. 12 2018.
- [81] Raji Atia and Noboru Yamada. Sizing and analysis of renewable energy and battery systems in residential microgrids. *IEEE Transactions on Smart Grid*, 7:1204–1213, 5 2016.
- [82] Guannan He, Qixin Chen, Chongqing Kang, Pierre Pinson, and Qing Xia. Optimal bidding strategy of battery storage in power markets considering performance-based regulation and battery cycle life. *IEEE Transactions on Smart Grid*, 7:2359–2367, 9 2016.
- [83] Mahmoud Roustai, Mohammad Rayati, Aras Sheikhi, and Ali Mohammad Ranjbar. A scenario-based optimization of smart energy hub operation in a stochastic environment using conditional-value-at-risk. *Sustainable Cities and Society*, 39:309–316, 5 2018.
- [84] Ang Xuan, Xinwei Shen, Qinglai Guo, and Hongbin Sun. A conditional value-at-risk based planning model for integrated energy system with energy storage and renewables. *Applied Energy*, 294:116971, 7 2021.
- [85] Miguel Asensio and Javier Contreras. Risk-constrained optimal bidding strategy for pairing of wind and demand response resources. *IEEE Transactions on Smart Grid*, 8:200–208, 1 2017.
- [86] Timur Saifutdinov, Charalampos Patsios, Petr Vorobev, Elena Gryazina, David Greenwood, Janusz Bialek, and Philip Taylor. Degradation and operation-aware framework for the optimal siting, sizing and technology selection of battery storage. pages 1–1, 12 2020.
- [87] Pavlo Krokmal, tanislav Uryasev, and Jonas Palmquist. Portfolio optimization with conditional value-at-risk objective and constraints. *The Journal of Risk*, 4:43–68, 3 2001.
- [88] S. D. Downing and D. F. Socie. Simple rainflow counting algorithms. *International Journal of Fatigue*, 4:31–40, 1982.

- [89] Junhan Huang, Shunli Wang, Wenhua Xu, Weihao Shi, and Carlos Fernandez. A novel autoregressive rainflow—integrated moving average modeling method for the accurate state of health prediction of lithium-ion batteries. *Processes*, 9, 2021.
- [90] Bolun Xu, Alexandre Oudalov, Andreas Ulbig, Göran Andersson, and Daniel S. Kirschen. Modeling of lithium-ion battery degradation for cell life assessment. *IEEE Transactions on Smart Grid*, 9:1131–1140, 2018.
- [91] Yuanyuan Shi, Bolun Xu, Yushi Tan, and Baosen Zhang. A convex cycle-based degradation model for battery energy storage planning and operation. *Proceedings of the American Control Conference*, 2018-June:4590–4596, 8 2018.
- [92] Chuanhai Chen, Zhaojun Yang, Jialong He, Hailong Tian, Shizheng Li, and Dongliang Wang. Load spectrum generation of machining center based on rainflow counting method. *Journal of Vibroengineering*, 19:5767–5779, 12 2017.
- [93] rainflow 3.1.1. <https://pypi.org/project/rainflow/>. Accessed: 2022-08-02.
- [94] Swasti R. Khuntia, Jose L. Rueda, and Mart A.M.M. Van der Meijden. Long-term electricity load forecasting considering volatility using multiplicative error model. *Energies*, 11, 12 2018.
- [95] <https://www.entsoe.eu/Technopedia/techsheets/enhanced-load-forecasting>. Accessed: 2022-09-01.
- [96] Wesley Cole, A. Frazier, and Chad Augustine. Cost projections for utility-scale battery storage: 2021 update. 6 2021.

